이학석사 학위논문

# Field Study of Orthopteran Escape Pathway's Response to Robotic Simulation of Visual Displays of Flush-Pursue Predators

# 로봇 모의실험을 통해 본 flush-pursuing 시각자극에 대한 메뚜기목의 반응

2013 년 8 월

서울대학교 대학원

생명과학부

문 종 열

# Field Study of Orthopteran Escape Pathway's Response to Robotic Simulation of Visual Displays of Flush-Pursue Predators

A Thesis presented by **Moon, Jong-Yeol**

Supervised by

Professor Dr. Hab. **Piotr G. Jablonski**

In partial fulfillment of the requirements for the degree of

**Master of Science, Biological Sciences**

August 2013

**Graduate School of Biological Sciences**

**Seoul National University**

# 로봇 모의실험을 통해 본 flush-pursuing 시각자극에 대한 메뚜기목의 반응

# Field Study of Orthopteran Escape Pathway's Response to Robotic Simulation of Visual Displays of Flush-Pursue Predators

지도교수 Piotr G. Jablonski

이 논문을 이학석사 학위논문으로 제출함

2013 년 8 월


서울대학교 대학원

생명과학부

문 종 열


문종열의 이학석사 학위논문을 인준함

2013 년 8 월

| | | |
|---|---|---|
| 위 원 장 | Eun Ju Lee | (인) |
| 부 위 원 장 | Piotr Jablonski | (인) |
| 위 원 | Bruce Waldman | (인) |

## Abstract

# Field Study of Orthopteran Escape Pathway's Response to Robotic Simulation of Visual Displays of Flush-Pursue Predators

**Moon, Jong-Yeol**
School of Biological Sciences
The Graduate School
Seoul National University

Some avian predators show unique behavior of "wing-flashing" to startle cryptic prey and to pursue it while it escapes. This helps in improving foraging rate. Even though the function of wing-flashing behavior has been well described as foraging strategy in several flush-pursuing birds, the foraging function is still little studied in the mockingbird. On the basis of former studies and observations, I hypothesized that the wing-flashing of mockingbird is important for foraging because it triggers escape behavior by stimulating escape pathways in the prey nervous system. Therefore, I tested

the effect of uniquely mockingbird's wing-flashing behavior on the response of neural pathways in the Orthopteran insects, which are known to be part of the mockingbird's diet. Mockingbirds perform "pause and hitch" wing display. I used a robot mimicking mockingbird to simulate the wing-flashing behavior. To find out the effect of "pause and hitch", I operated the robot in two modes: one was a typical wing-flashing with hitches often observed in mockingbirds and the other was a full wing-flash without hitches. As a prey, I used a grasshopper that inhabit the desert in Arizona - the habitat of mockingbirds. I recorded the spiking activity in the DCMD neuron of grasshoppers, which is mainly sensitive to looming objects approaching directly toward to prey. Those neurons are connected to the motor neurons that induce escape jump or flying in response to visual stimuli. I found that there was delay from the stimulus of robot to the response of neuron. Because of this delay, largo portion of the spiking activity appeared during the pause in the wing movements. It is expected that grasshopper would often escape during this pause period between wing opening movements. If so then it is beneficial to the mockingbird because it may be easier to start a fast pursuit after the prey when no other wing movements occur (in the pause stage). Moreover, the spiking activities show strong increase right from the very start of the wing flash movements. Hence, when the robot performed several hitches, the increase of spiking activity in the neurons appeared several times during the robot wing display. This increases the chances that escape is

triggered because escape occurs each time when activity reaches/passes through a hypothetical threshold.

In summary, the DCMD activity was triggered in response to the robotic wing display and the timing of the neurons' response in relation to the wing flash timing suggested specific adaptive explanations for the "pause and hitch" nature of the wing flash display.

**Keywords : Wing-flashing, Flush-pursue, Pause and Hitch, Neural pathway, Visual stimuli, Escape**

***Student Number : 2010-23108***

# Table of Contents

# List of Tables

# List of Figures

# 1. Introduction

Predator adaptations to find and attack a prey and prey adaptations to avoid predation are often presented as classical outcomes of coevolutionary arms race (Dawkins 1982, Dawkins and Krebs 1979). Evolutionary arms races in two –species systems of prey and predator indeed occur and they reflect natural selection for ever increasing efficiency of predators to capture the prey and natural selection on prey for ever increasing abilities of prey to avoid predation. The comparison to arms race is a simplification that may explain evolution in predator-prey systems comprised of one predator and one prey, but in more complex systems with multiple predator species some additional evolutionary processes may be at play (Abrams 1991, Matsuda *et al* 1993, Matsuda *et al* 1996). For example some predators can capitalize on prey adaptations to avoid other predators. These predators exploit prey antipredatory adaptations such like for example adaptations to initiate escape in response to approaching predators. Because these predators are usually encountered by prey much less often than the dominant predators in a given system, the prey species maintain their escape behavior against common predators rather than evolving a new strategy in response to the less common predators. Therefore the rare strategies of predators to exploit prey

antipredatory adaptations can persist in multispecies ecological systems (Charnow E. L. *et al*. 1976, Jablonski 1999, Magurran 1990).

The best well-known exploitation of prey escapes is that predators flush the prey and chase it along the escape trajectory. These flush-pursuing predators could increase frequency of successful attacks by exploiting prey escape behavior that evolved to avoid predation from other predators (Galatowitsch and Mumme 2004, Jablonski 1999, 2002, Jablonski and McInerney 2005). This strategy has been observed in several taxa including human (e.g. falcons: Hedenstrom 2001, gulls: Hendricks and Hendricks 2006, Tinbergen 1960, humans: Catania 2008, snakes: Catania 2012, turtles: Kaufmann 1986). Especially in case of birds, this exploitive behavior is expressed as wing-flashing that triggers prey escapes (Table 1) (Ali 1962, 1977, Ali and Ripley 1973a, b, Batts 1962, Beehler *et al* 1986, Cramp 1992, Ficken and Ficken 1962, Fleming *et al* 1979, Hailman 1960, Halle 1948, Haverschmidt 1953, Horwich 1965, Hundley 1963, Jablonski 1999, MacKinnon and Philips 1993, Moynihan 1962, Pizzey 1980, Ridgley and Tudor 1989, Robinson and Holmes 1982, Sherry 1984, Whitaker 1957). For example, in order to flush the prey, the painted redstart (*Myioborus pictus*) spread their wings and tail suddenly in a certain direction. When the bird displays the series of flushing behavior, some of preys (e.g. flies) flush from the substrate (Jablonski 2002, Jablonski and Strausfeld 2001) on which they are relatively inconspicuous. Once they jump they suddenly reveal their

presence to the predator. Then redstarts can chase and attack the flushed insects (Jablonski and McInerney 2005). It has been suggested that this flush pursue technique is based on exploitation of responses of a simple neural pathway that mediates visually triggered escape behavior in Dipteran prey: the Giant Descending Neuron pathway comprising a bundle of neurons some of which are believed to respond to looming stimulus (Jablonski and Strausfeld 2000, 2001). Although electrophysiological recordings from dipteran insects in response to the simulations of foraging flush-pursuing birds are consistent with this idea (Jablonski unpublished), many aspects of the dipteran escape pathway are much less understood than the classical model for such escape behavior: locust. Locusts are not a typical prey of the redstarts but they are quite common (Beal *et al* 1941, Derrickson and Breitwisch 2011) in diet of the Northern mockingbird (*Mimus poyglottos*) - another bird species that also seems to use the flush-pursue technique.

Northern mockingbirds (*Mimus polyglottos*), similar to redstarts, also spread their wings (i.e. wing-flashing behavior) in a specialized manner, but this behavior appears to be used in a larger variety of contexts. Wing-flashing behaviors of mockingbirds, especially in young birds, occurs in response to being in an unfamiliar environment (Horwich 1965, Laskey 1962). In adults, the behavior can be used in agonistic interactions (Selander and Hunter 1960), in displays towards predators (Dhondt and Kemink 2007) and in foraging behavior (Hailman 1960). In the latter the use the wing-flashes appear to help

in foraging in some studies (Hailman 1960) but not so in other studies (Burtt *et al* 1994, Hayslette 2003). Nevertheless the use of wing displays during foraging is well known and the hypothetical explanation assumes that the wing displays cause insect prey to move, including escapes, which helps the predator in detecting the prey.

In this thesis, I evaluate the idea that wing-flashing is used by mockingbirds to visually stimulate specific neuronal pathways that mediate escape behavior in prey. This is the underlying assumption of the hypothesis that flush-pursuers exploit relatively simple visually triggered escape reaction in prey in order to increase predation efficiency (Jablonski and Strausfeld 2000, 2001). Hailman(1960) presented data suggesting that wing-flashing of the mockingbird increases the efficiency of foraging.

My aim was to record the electrophysiological response in neuronal escape pathway of Orthopteran prey in response to mockingbird displays. Descending contralateral movement detector (DCMD) neuron is believed to play a role in triggering escape jumps in response to visual looming stimulus approaching directly toward the eye (Rind and Simmons 1992, 1999, Santer *et al* 2006, 2008). Looming is defined by expanding object on the prey retina and Orthopteran escape pathway specifically respond to looming that is characteristic for fast approaching objects such like attacking predator or falling stone, etc. In general, the accelerating movement of image edges of an approaching object across retina is one of the crucial basic elements of the

looming stimulus that is important for triggering activity in the LGMD/DCMD escape pathway (Rind and Bramwell 1996). I hypothesized that movement of mockingbird wings during their wing-flash displays may exploit this visual sensitivity of prey, and therefore may be used to trigger escape behavior. Wing-flashing behavior, comprising fast expansion of both wings while the bird is stationary, is an effective way to mimic image expansion normally associate with a fast attack at a prey.

I conducted experiments using a robot that mimics the wing-flashing behavior of mockingbirds to record prey responses. For examining the preys' responses, I looked at spiking activity of the descending contralateral movement detector (DCMD) of wild grasshoppers in their natural habitat where mockingbird hunt them.

**Table 1.** Examples of flush-pursuing birds.

| English name | Family | Species |
|---|---|---|
| Northern Mockingbird | Mimidae | *Mimus polyglottos* |
| Chalk browed Mockingbird | Mimidae | *Mimus saturninus* |
| Tropical Mockingbird | Mimidae | *Mimus gilvus* |
| Floreana Mockingbird | Mimidae | *Nesomimus trifasciatus* |
| Gray Catbird | Mimidae | *Dumetella carolinensis* |
| Brown Thrasher | Mimidae | *Toxostoma rufum* |
| White-throated Fantail | Rhipiduridae | *Rhipidura albicollis* |
| White-browed Fantail | Rhipiduridae | *Rhipidura aureda* |
| Dimorphic Fantail | Rhipiduridae | *Rhipidura brachyrhyncha* |
| Wilie wagtail | Rhipiduridae | *Rhipidura leucophrys* |
| Slate-throated Whitestart | Parulidae | *Myioborus miniatus* |
| Collared Whitestart | Parulidae | *Myioborus torquatus* |
| American Redstart | Parulidae | *Setophaga ruticilla* |
| Yellow-browed Warbler | Phylbscopidae | *Phylloscopus inornatus* |
| Green Warbler | Phylbscopidae | *Phylloscopus nitidus* |
| Greenish Warbler | Phylbscopidae | *Phylloscopus trochiloides* |
| Pygmy Flycatcher | Muscicapidae | *Muscicapella hodgsoni* |
| Ruddy-tailed Flycatcher | Tyrannidae | *Terenotriccus erythrurus* |

# 2. Materials and Methods

## 2.1. Study Species

Northern mockingbird (*Mimus polyglottos*)

Northern mockingbird is an American bird species that inhabits mountains, grasslands, and deserts (Figure 1, 6). The distribution of the mockingbird ranges from North America to Mexico. This species is omnivorous and hunt insects. This bird shows a unique behavior called “wing-flashing behavior” (Figure 1). While walking or running around, it stops abruptly and spread its wings by step-by-step process (display with pauses), then closes its wings. The wing-flashing display of mockingbird usually have 1~5 hitches and 3 or 4 hitches are the most commonly observed (Dhondt and Kemink 2007, Hailman 1960, Horwich 1965, Rich 1980), This behavior has been known as ‘flush-pursuit’ display and is regarded as an adaptation of mockingbirds to hunt the ground dwelling insects. If a bird detects any insect that may be flushed or caused to move by this display, the bird rushes toward the prey in an attempt to capture it. And the birds repeat the foraging displays immediately after hunting.

**Figure 1.** Mockingbird and its wing display.

## 2.2. Description of the wing display of the mockingbird

I used video clips of foraging mockbirds to characterize the wing-flash behavior during foraging. The change of wing tip position during a wingflash was recorded in a coordinate system with the center at the mockingbird head set to the origin (coordinates 0,0). Wing flashes were measured from only those clips that represented a frontal of rear view of the mockingbrid. The average coordinates of the wing tip position in two dimensions were measured to show the spreading wing movement. Timing of the wingflash movements was measured from all clips (filmed with 25 or 30 fps) regardless of the orientation of the birds (see table 2).

## 2.3. Description of the robotic mockingbird

To study whether "wing-flashing behavior" actually enhances the foraging performance of mockingbirds, I used the robot that mimics the shape and behavior of real mockingbird. The robot was developed by collaboration with Prof H. Moon at the Sungkyunkwan University. The robot generally mimicked the shape of birds (Figure 4). Specifically this robot performs wing-flashing behavior by either continuously or step-by-step (Figure 4). The robot has metal wing skeletons and detachable wings made by paper that could be flashed like real mockingbird. Then we additionally made the body and head by art clay and paint it to mimic the actual color of mockingbird viewed from the front side. The robot is larger than real mockingbird.

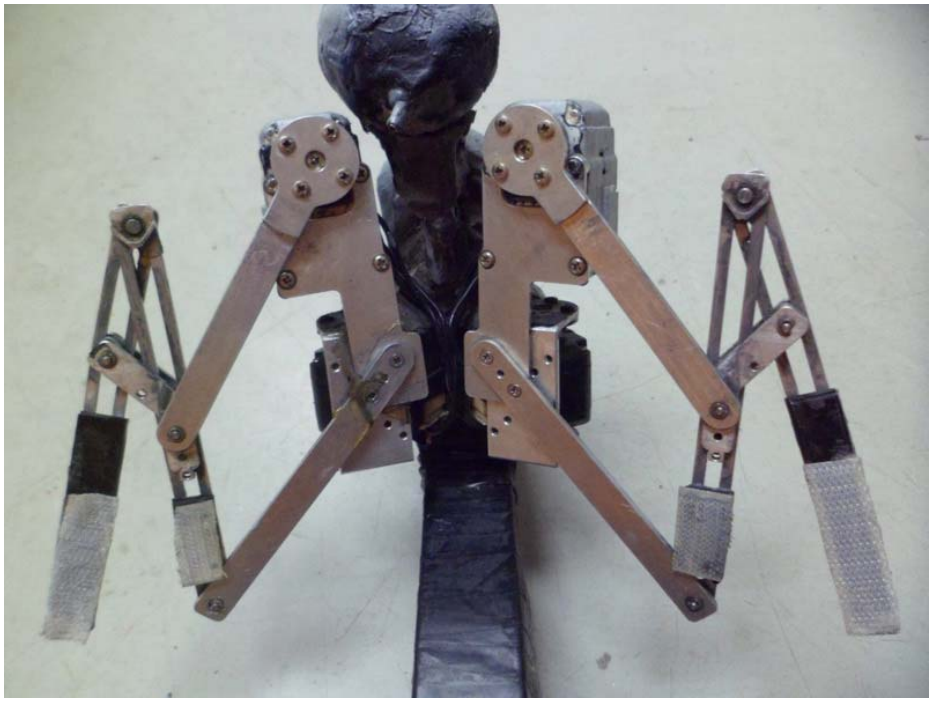

**Figure 2.** Skeleton of robot.

**Figure 3.** Paper wings.

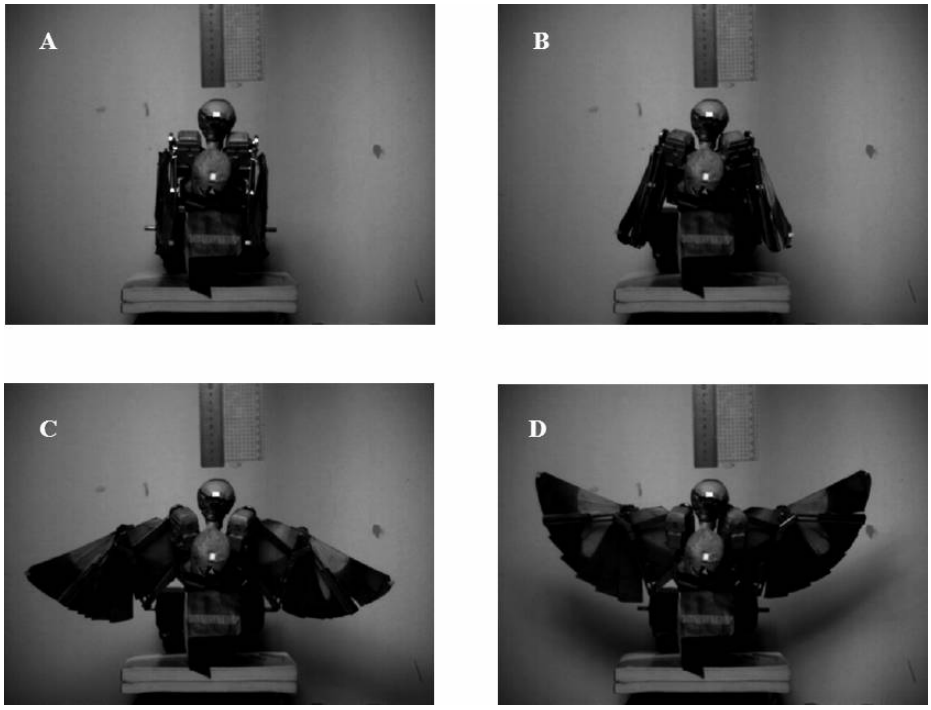


**Figure 4.** Wing display of robot with 3 hitches and pauses.
A: before moving, B: first pause, C: second pause, D: last pause.

We used the control board to operate the mockingbird robot (Figure 5). The robot has a wire behind the bottom of the body to connect to control board. The other side of the control board has a connecting piece to a battery. Another side can connect to a computer. Robot is powered from battery through a control board and controlled by Host program installed in computer. The program named Mockingbird Host Program was provided with the robot from the students at Sungkyunkwan University. We used the Mockingbird Host Program only for displaying wings of the robot by either of two ways: continuously or with pauses. Executing Host program, I could manipulate the number of pauses in a display of wings, wing speed of the display, duration of each pause during display. I measured the actual wing display speed and duration of pauses in real mockingbird, and applied these measurements to mockingbird robot. So the wing speed of display and the duration of each pauses in robotic mockingbird followed those of real mockingbirds. The main focus of this experiment is how 'hitch and pause' display of mockingbird affects the response of prey. Therefore I used two types of display (continuous display and display with three pauses) and other settings in the program were never changed.

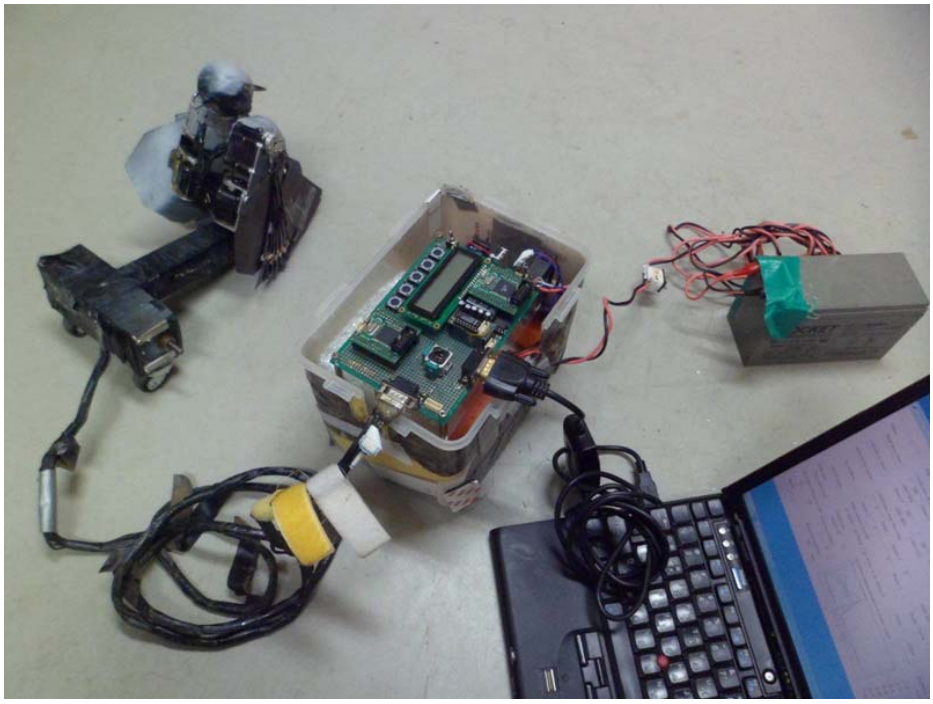

**Figure 5.** Equipment full sets (control board, robot, battery, laptop).

## 2.4. Study site, prey species and escape neurons in Orthoptera

This field study was conducted at or near the South Western Research Station (SWRS) in Arizona, U.S.A. on July 2010, June 2011.

***Pallid-winged grasshopper (Trimerotropis Pallidipennis) as a prey species***

To record neural response of preys in response to mockingbird's wing-flashing display, I used Pallid winged grasshopper (*Trimerotropis Pallidipennis*). I chose grasshoppers to study since they are one of the main diet of mockingbirds (Beal *et al* 1941, Derrickson and Breitwisch 2011), and neural mechanisms which elicit the escape responses in Orthopterans have been well understood.

There have been many studies that revealed the activity of neurons and how the neural activity mediates escape jump in response to visual looming objects. The spiking activity in the 'lobula giant movement detector' or LGMD is produced as a result of visual stimulation of insect retina by moving edges of a looming stimulus (Burrows and Rowell 1973, Burrows 1995, 1996, Dawson *et al* 2004, Gabbiani *et al* 2002, Gray *et al* 2001, Heitler and Fraser 1993, Rind and Bramwell 1996, Simmons 1981, Simmons *et al* 2010). Another identified visual neuron, the 'descending contralateral movement detector' or DCMD receives synaptic input from the LGMD (Gray

*et al* 2001, Rind 1984, Rind and Simmons 1992, Simmons and Rind 1992). The LGMD/DCMD neurons are the largest visual neurons (Rind and Simmons 1992) and they respond vigorously to images of objects that approach directly towards the insect viewing them (Hatsopoulos *et al* 1995, Judge and Rind 1997, Rind and Simmons 1992, Simmons *et al* 2010). Although the details are not yet known, the Orthopteran DCMD neurons make connections with motor neurons and interneurons that are involved in triggering prey escape behavior such like flying or jumping (Burrows and Rowell 1973, Simmons *et al* 2010).

## 2.5. Recording neural response of Orthopteran prey in response to the robotic wing displays

I performed electrophysiological recording of the DCMD activity in grasshoppers while the robot gave its visual display.

Grasshoppers were collected from the desert and experiments were done around the collect site and finished within daytime. I successfully recorded the neural response of 8 grasshoppers (1 juvenile grasshopper and two adults in 2010, five adult grasshoppers in 2011).

**Figure 6.** A photo of the habitat of the grasshopper and mockinbirds.

**Figure 7.** Experimental setting in the field.

First, I fixed a grasshopper using wax (Figure 8). I removed the antennae and front legs and covered one eye by wax. Then I dissected the soft part of the insect, unsclerotized cuticle of a cervix between head and thorax to expose the ventral nerve cord (Figure 9). Then I removed floating matters, which can potentially create noises in neural signal, to get neural responses clearly. To prevent drying (which causes death of the grasshopper), I dropped saline solutions on the dissected part until I finished the experiment.

Right after dissection, a pair of hook electrodes was dipped on the dissected cervical connective (Figure 11).

**Figure 8.** Grasshopper fixed using wax with only one eye facing the area where the robotic stimulus was dipslayed agains natural background.

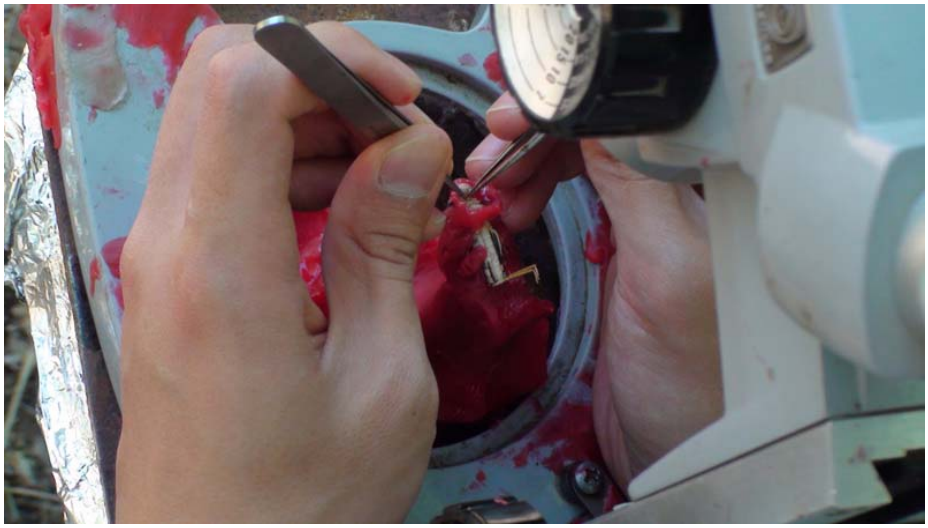

**Figure 9.** Dissection cervix of grasshopper with tweezers and scissors.

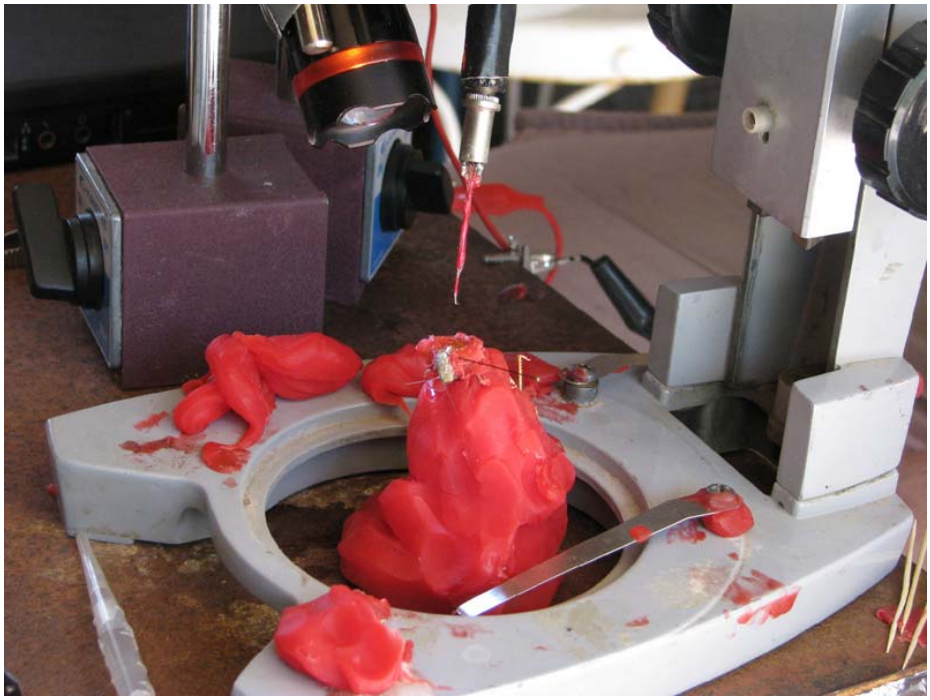

**Figure 10.** Grasshopper is about to be conneted to electrodes.

The recording setup consisted of a pair of hook electrodes, connected to the miniature differential preamplifier MPA8I, which was connected to the portable USB ME16 amplifier from Multichannel Systems. Extracellular silver wire hook electrodes were wrapped around the contralateral chord (i.e. for recording from the right eye the electrodes monitored signals from the left chord). The program MC_Rack was used to record the signals.

During the extracellular recordings from the axon, a computer screen shows DCMD spikes. The visual stimuli (wing-display of robot) stimulated the neural signals in DCMD neural circuits.

In order to link the exact timing of the robot wing display with the recorded neural response, we video recorded wing display of the robot while recording neural responses. We synchronized the time in the video and the time in the neural recording. Video recording of the displaying robot was done with the camcorder (HDR-SR1, SONY®, 33fps).

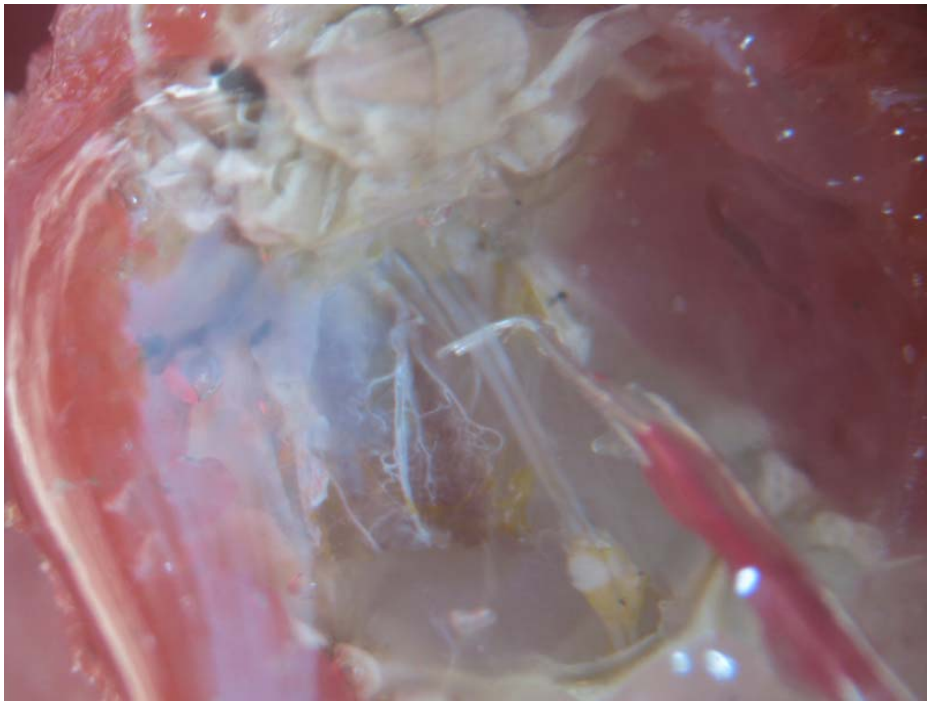

**Figure 11.** Connection a hook electrode tip and the ventral nerve cords.

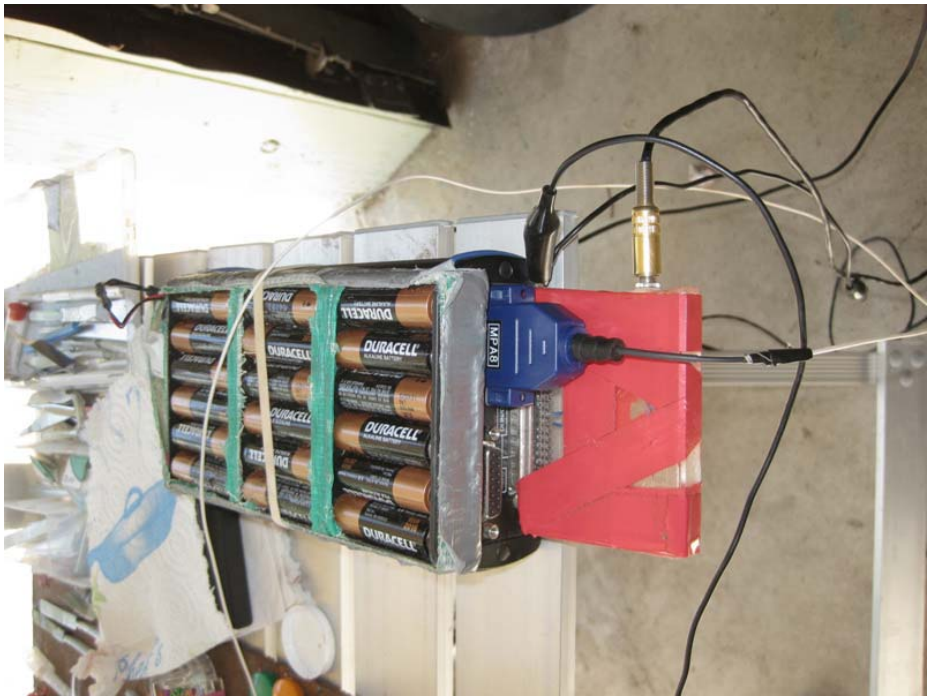


**Figure 12.** The battery operated USB ME16 amplifier set for the experiments.

## 2.6. Recording the robot display

Mockingbird robot was positioned at the same height as a grasshopper's eye. Then I operated the robot to display wings, and the DCMD activity of the grasshopper was recorded. In order to mimic mockingbird wing flashing display at various distances from prey, we used several distances between the grasshopper's eye and mocking bird robot. The display of robot began at 2.4m from a grasshopper at the first time, then become closer to 1.2, 0.6, 0.3, 0.15m in sequence. We calculated how the robot would be viewed by grasshopper at these distance.

**Figure 13.** Display of a robot viewed by the camera located behind the grasshopper.

## 2.7. Movement of a mockingbird robot in a prey's visual field

It is well know that approaching objects stimulate the escape behavior of insects. In 2-dimensional point of view of insects, the approaching object can be re-described as the increment in the size of the object. Studies on insect neurons and escape behavior have suggested that the angular speed of the increasement in size (which usually corresponds to the approaching of an object) and its changes are correlated with the intensity of spiking in the DCMD pathway and they are crucial to elicit escape responses (specifically ever increasing angular speed is the feature that stimulates DCMD pathway and triggers the escape).

Therefore I decided to analyze the angular size, speed and acceleration of the wing display of robotic mockingbirds from the point of view of grasshopper, and how it is related to the neural response. To analyze how display of the wings of robotic mockingbirds are viewed by grasshoppers, I video-recorded the display of the robot wings. I used a high speed camera (250fps, lens: TV ZOOM LENS, M6Z 1212 – 3S, 12.5 – 75mm F1.2 (www.edmundoptics.com)) for recording. The camera lens faced the display of robot as grasshopper did. The distance from the center of the robot to the lens was 1.8m. I put a ruler with robot in the same distance from the camera to measure the actual distances. Like the field experiments, recording was

conducted on two types display (with and without hitch). Each type of display was performed three times so I got three recordings of each display respectively. For analysis, I averaged the values in each movie.

I used speed the expansion of the distance between the wing tips (Figure 4) as an approximation of the speed of the wing display. I extracted the x, y coordinates of the wing tips frame by frame, and calculated how fast the tip moved during display of the robot. I transformed pixel values to standard units (cm). From this data, I calculated speed of the wing tips during display and acceleration of the wing tips during display, and angular speed and acceleration of the wing tip movement from the point of view of the grasshopper. The left wing and the right wing were calculated separately and averaged. The method is described below.

***Measuring the angular speed of increasement in wing tips from the point of view of the grasshopper***

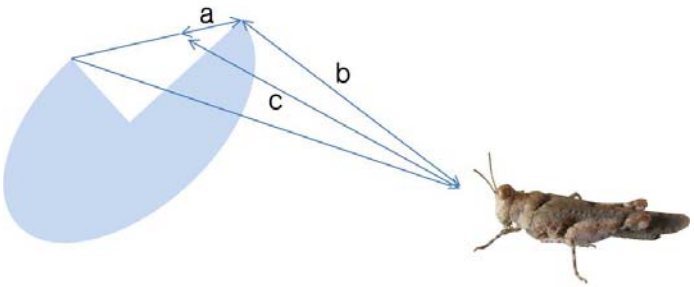


**Figure 14.** Angular size between the left wing tip and the right wing tip.

(1) b = distance from grasshopper's eye to a wing tip

(2) c = distance from grasshopper's eye to a robot directly

(3) a = half distance between wing tips

(4) angular size = $2\cos A = (b^2 + c^2 - a^2) / 2bc$

(5) angular speed = radian / 0.004s  (1s = 250 frames)

(6) angular acceleration = angular speed / 0.004s

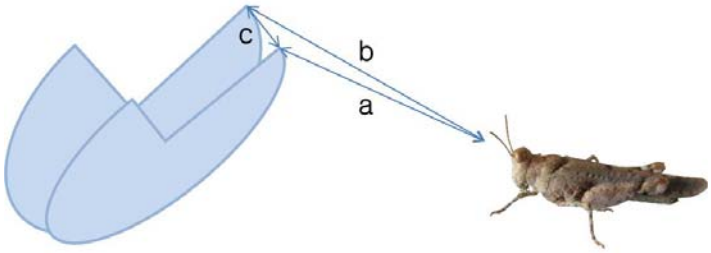


**Figure 15.** Angular size between the former wing tip and the later wing tip.

(1) distance from the center of robot to a wing tip

$= \sqrt{}$ (x-coordinate of a wing tip)$^2$ + (y-coordinate of a wing tip)$^2$

(2) a = distance from a grasshopper's eye

to a wing tip at the former frame

$= \sqrt{}$ (distance from a grasshopper's eye to robot directly)$^2$

+ (distance from the center of robot to a wing tip)$^2$

(3) b = distance from a grasshopper's eye to a wing tip at the later frame

(4) c = distance of a wing tip movement from the former frame

to the later frame

$= \sqrt{}$ (x-coordinate of later frame – x-coordinate of former frame)$^2$

+ (y-coordinate of later frame – y-coordinate of former frame)$^2$

(5) angular size = $\arccos (a^2 + b^2 - c^2) / 2ab$

## 2.8. Recording neural response of Orthopteran species in response to looming objects

Since DCMD activity is higher in response to approaching stimulus (Gabbiani e al 2004, Gabbiani et al 2005, Gabbiani and Krapp 2006, Rind and Simmons 1992, 1997, Simmons and Rind 1992), I tried to compare the response of grasshoppers to looming object with the response of grasshoppers to robotic display. I used a hand controlled approach a black disk to a grasshopper's eye directly. The disk was 30cm in diameter made of hard paper and a modified photographic tripod was used as a support (Figure 16).

**Figure 16.** Looming experiment.

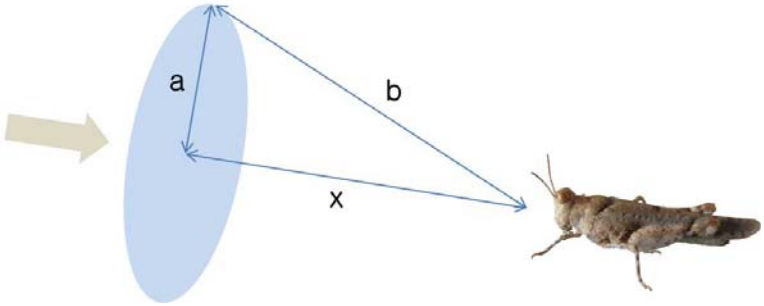


**Figure 17.** Angular size between the edges.

(1) a (radius of a disk) = 0.15m

(2) x = distance from a grasshopper's eye to the center of a disk

(3) b (distance from a grasshopper's eye to the edge of a disk)

$$= \sqrt{x^2 + 0.15^2}$$

(4) b = c

(5) angular size = $\cos A = (b^2 + c^2 - a^2) / 2bc$

## 2.9. Analyzing electronic signal data

I analyzed the neural spike data using MC_Rack, MC_Data Tool and Spike2 software. First, the neural spikes were transformed to the analyzable files using MC_Rack and MC_Data Tool. Then I used Spike2 to analyze the patterns in spikes in response to visual stimuli.

Spike sorting process was conducted in Spike2 (version 5, Cambridge Electronic Design, Cambridge). At first, I filtered the electronic signals to reduce electric noise using band-pass filter. While filtering I set two types of threshold: high and low threshold. The high threshold filtered all of the noises by setting high threshold (thus relatively safe from electric noises, but with a risk of detecting some real signals). In contrast, the low threshold set the low level of threshold (thus increase the chance of false positive detection of signals, but relatively safe from losing real signals during filtering).
Then I counted how many spikes were appeared in response to each wing display of robots.

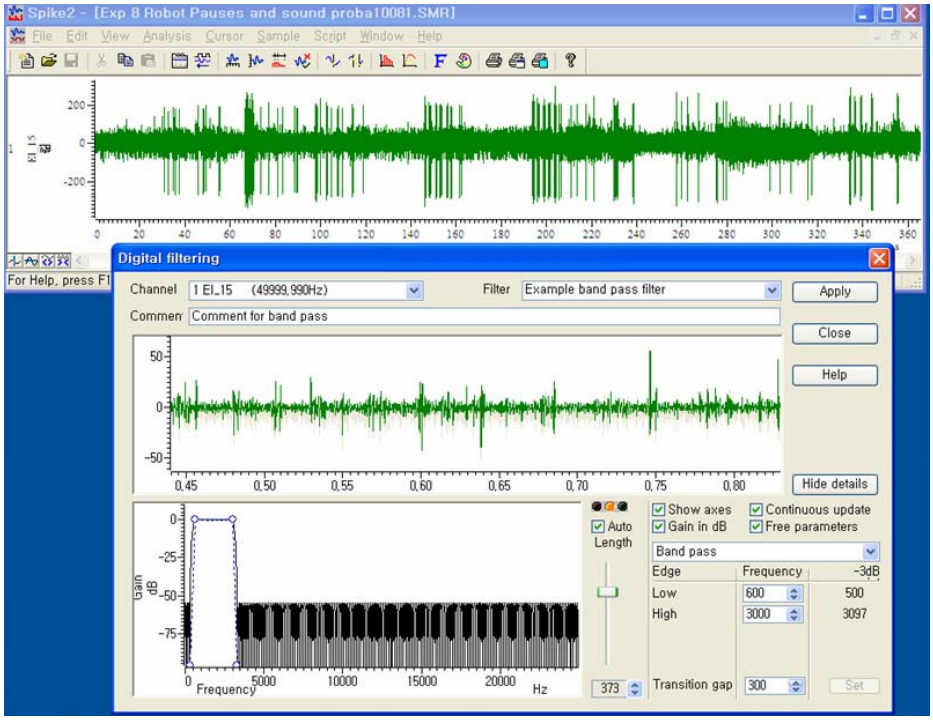


**Figure 18.** Processing of filtering.

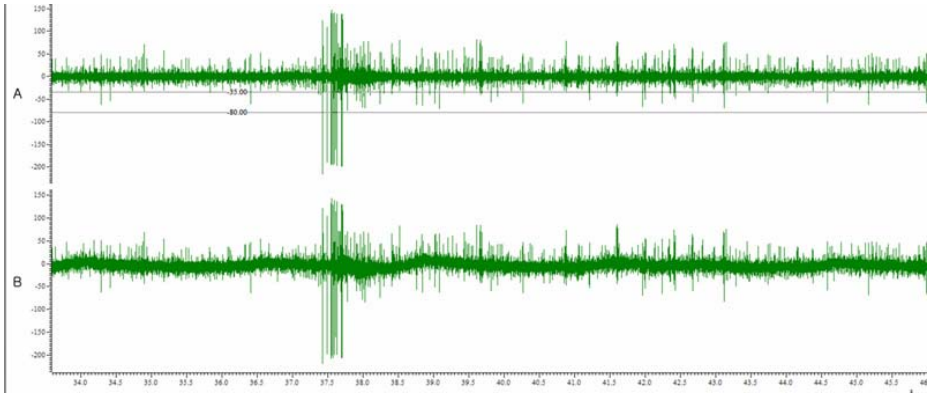


**Figure 19.** Original signal (B) and filtered signal with thresholds (A).

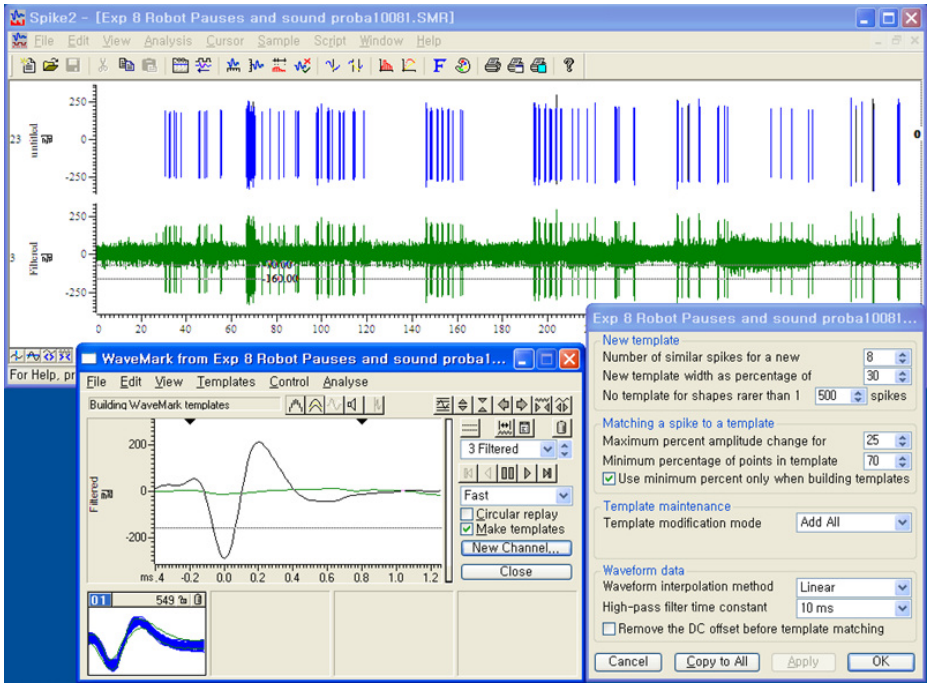


**Figure 20.** An image showing the Spike2 software. Parameters of template (bottom of the right side), Template (bottom of the left side). Threshold levels are different in each signal files but the width is 1ms in the all signal. The whole response signal of a grasshopper from the experiment with hitch (green signal) and show the spikes beyond the wide threshold level (blue signal).

The Figure 19 shows both the original signals before filtering and the filtered signals. Typical shape of the spikes is shown in Figure 20. We counted all the spikes shaped like this spike using Spike2 software.

The valid spikes which passed through the threshold level (blue signal in the figure in Figure 20) were counted in each bin (bin width =0.02s) and exported to excel sheet where they were further analyzed. For each recording I have sorted spikes two times: using high threshold and using low threshold. High threshold criterium means that only the largest spikes were counted. Low threshold criterium means that in addiction to the largest spikes the spikes with smaller amplitude were also counted, but the background smaller spikes were always ignored (Figure 19).

# 3. Results

## 3.1. Comparison of the neural spikes in response to looming objects and spikes in response to robotic display

For those looming disk approaches that fairly accurately imitated the increasing angular speed of a simple looming stimulus (approaching dark disk) the approach caused a series of large spikes (Figure 21)

The spike shape of the signal from the looming experiment is similar to the spike shape from the experiment of a robot display that simulated a real bird's display. (Figure 21C, D) indicating that the signal recorded in response to the simple looming most likely originated from the same neural units as in the experiments with robotic wing displays. Considering the shape and that these are the largest spikes produced by the grasshopper, and following the procedures established by neurophysiologists who study the DCMD pathway, we assume that, as intended, we have recorded the response of the DCMD pathway. In general, these results indicate that the stimulus from the simple looming object triggered the same neural pathways as the stimulus from the robot displays. Additionally we have confirmed that it is the visual element rather than sound that causes the spike activity in response to the robotic display.

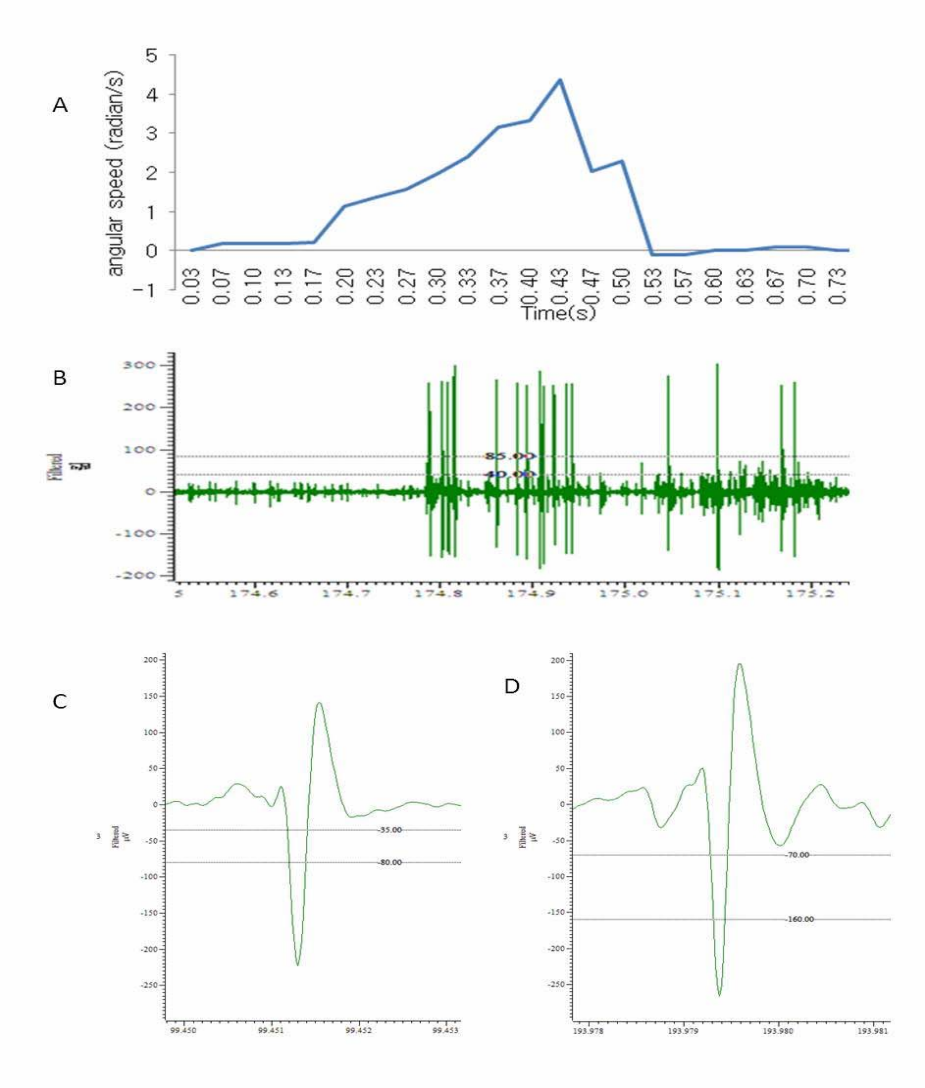


**Figure 21.** A: angular speed of a looming object (30cm diameter black thin paper circle) between the edges of the object in the view of a grasshopper's eye. B: DCMD spikes of grasshopper to the looming object. C: one spike from the signal response to the looming object. D: one spike from the signal response to the robot display with hitch.

## 3.2. Wing movement of mockingbird

Table 2 shows the duration time of each pauses and hitches during the wing-flashing and Figure 22 shows the coordinates of the wing tips.

**Table 2.** Mean time durations (sec; with Standard errors) of the consecutive hitches and pauses in the mockingbird's wing display for four types of displays categorized by the number of wing hitches performed by the bird (one hitch display, two-hitch display, three-hitch display and four-hitch display).

| Stage | Nr hitches in the display | Mean duration (s) | Number of displays analyzed | SE (s) | Minimum (s) | Maximum (s) |
|---|---|---|---|---|---|---|
| Hitch1 | 1 | 0.097 | 11 | 0.016 | 0.035 | 0.207 |
| Hitch1 | 2 | 0.101 | 16 | 0.012 | 0.035 | 0.200 |
| Hitch1 | 3 | 0.111 | 12 | 0.019 | 0.033 | 0.241 |
| Hitch1 | 4 | 0.127 | 2 | 0.007 | 0.120 | 0.133 |
| Hitch2 | 2 | 0.115 | 17 | 0.020 | 0.067 | 0.414 |
| Hitch2 | 3 | 0.084 | 12 | 0.011 | 0.033 | 0.120 |
| Hitch2 | 4 | 0.084 | 3 | 0.018 | 0.067 | 0.120 |
| Hitch3 | 3 | 0.091 | 12 | 0.009 | 0.033 | 0.120 |
| Hitch3 | 4 | 0.096 | 3 | 0.016 | 0.067 | 0.120 |
| Hitch4 | 4 | 0.096 | 3 | 0.016 | 0.067 | 0.120 |
| Pause1 | 1 | 0.137 | 11 | 0.023 | 0.069 | 0.310 |
| Pause1 | 2 | 0.144 | 16 | 0.016 | 0.069 | 0.345 |
| Pause1 | 3 | 0.126 | 12 | 0.012 | 0.069 | 0.200 |
| Pause1 | 4 | 0.073 | 2 | 0.007 | 0.067 | 0.080 |
| Pause2 | 2 | 0.108 | 16 | 0.009 | 0.035 | 0.172 |
| Pause2 | 3 | 0.148 | 12 | 0.007 | 0.120 | 0.172 |
| Pause2 | 4 | 0.129 | 3 | 0.004 | 0.120 | 0.133 |
| Pause3 | 3 | 0.211 | 9 | 0.027 | 0.133 | 0.400 |
| Pause3 | 4 | 0.153 | 3 | 0.010 | 0.133 | 0.167 |
| Pause4 | 4 | 0.107 | 2 | 0.027 | 0.080 | 0.133 |

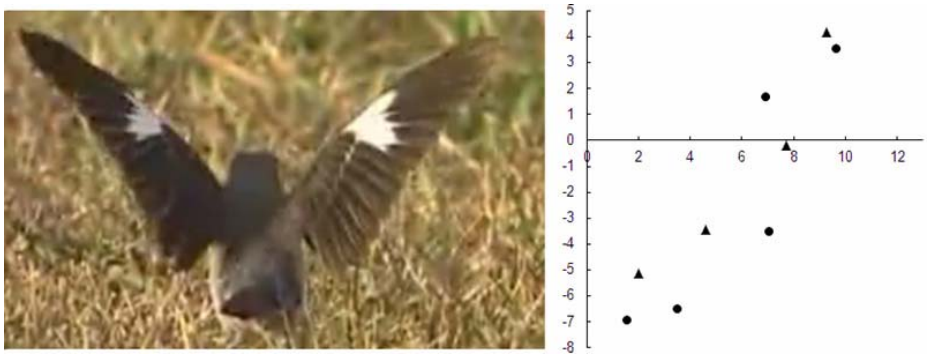


**Figure 22.** The wing tip position change. With 3 hitches (triangle), with 4 hitches (round). The coordinates of the top of head is (0,0). Unit: cm

## 3.3. Description of the three-hitch wing movement by a robot and electrophysiological response of prey

### 3.3.1. Wing movement

Because the robotic model is larger than the mockingbird, the range of motion as measured in absolute distances (cm) awas wider than that of a real bird.

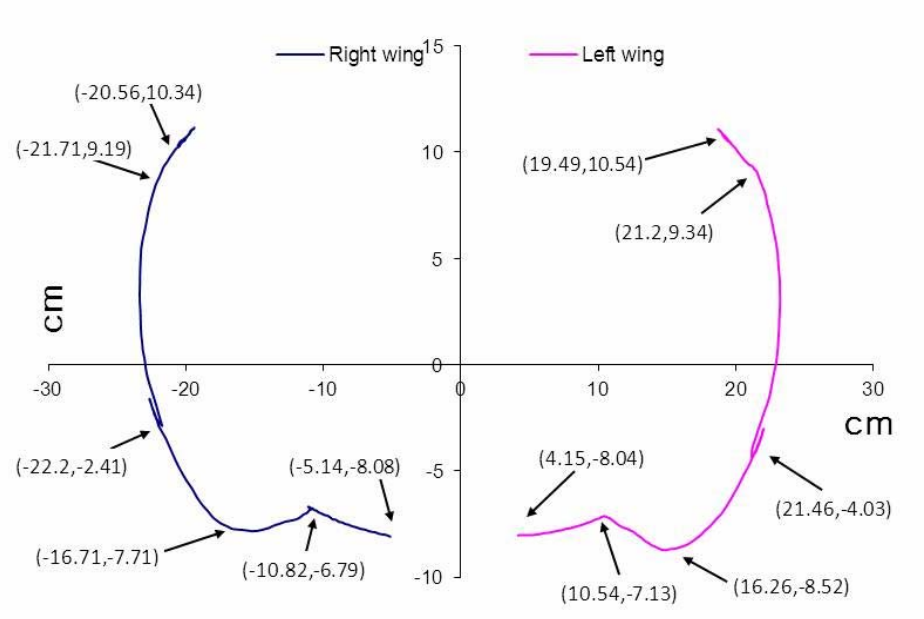


**Figure 23.** The movement of wing tips of the robot during display (left wing and right wings respectively) The numbers indicates x,y, coordinates of the wing tips (in cm) when I set the center of a robot (the white patch of Figure 3.) area as the origin. The time interval between the marked coordinates is 41 frames. The time interval beween frames is 0.004 ms.

### 3.3.2. Distance between the left wing tip and the right wing tip

The increasing distance between the wing tips during the wing flash is used here as a very general approximation of how the object (robot) image increases in size sidewise as the wings are being opened. In this sense it is a very approximate analog of looming (assuming that most increase in size is due to sidewise expansion of the wings). We chose this variable for the easiness of measurements but ideally a change in surface area covered by the image of the robot should be used. The distance between left and right wing tip was calculated based on the x,y coordinates of the both wing tips. The distance increased gradually but it shows a tendency to decrease in the final part (Figure 24A).

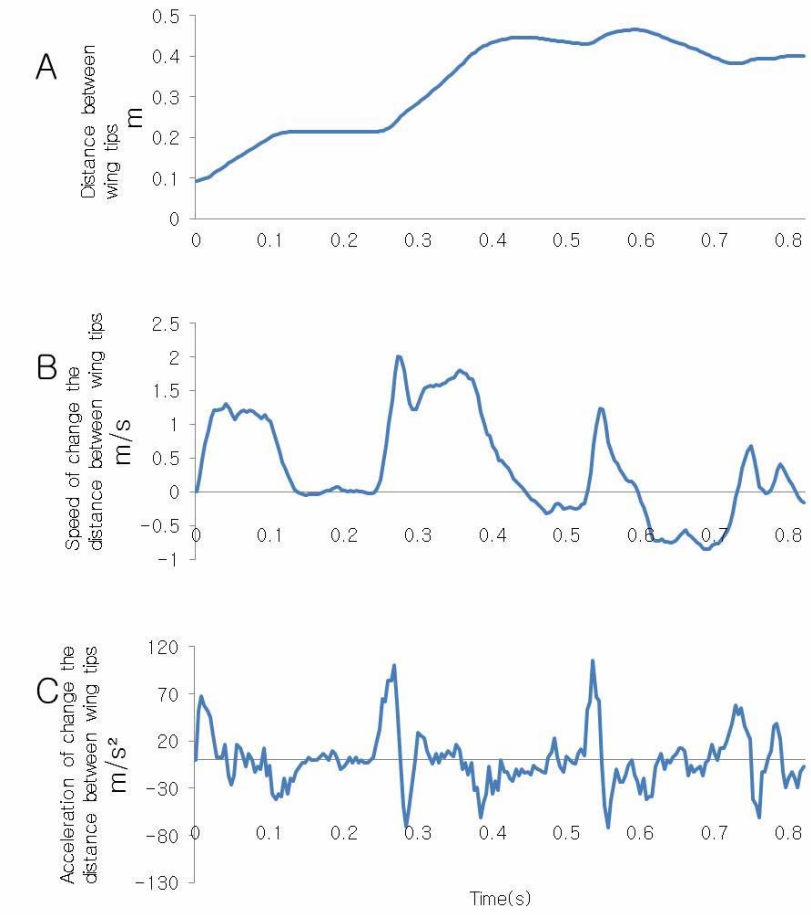


**Figure 24.** The distance between wing tips (A), speed (B) and acceleration (C) of wing expansion (change of distance per time unit) of the robot display represented in linear coordinates assuming that the wing expansion occurs in the two-dimensional plane corresponding to the image in the high speed camera (250fps. lens: TV ZOOM LENS, M6Z 1212 – 3S, 12.5 – 75mm F1.2(www.edmundoptics.com)) is 1.8m. A: distance between the wing tips of robot with time. x-axis: time(s) y-axis: distance(cm) B: speed of change of distance between wing tips. x-axis: time(s) y-axis: speed(cm/s) C: acceleration of change of distance between wing tips. x-axis: time(s) y-axis: acceleration(cm/s²)

### 3.3.3. Coordinates of the wing tip according to time

The movement of the wing tips are used here as a general index of the movements of the object edges in the image that is perceived by the insect. From the starting moment of wing opening until the moment of opening completely, the movement occurs horizontally (along the x-axis much more than y-axis) in the first part but it becomes more vertical (larger according to y-axis) in the second part. This general characteristic of wing movement is also present in the mockingbird movement albeit to a lower degree (compare Figure 23 with Figure 22). In the figure A, B, in the three hitches, wing tip mostly traveled along the x-axis in the first hitch but the vertical speed along the y-axis gradually increased during the second hitch and especially the thrid hitch.

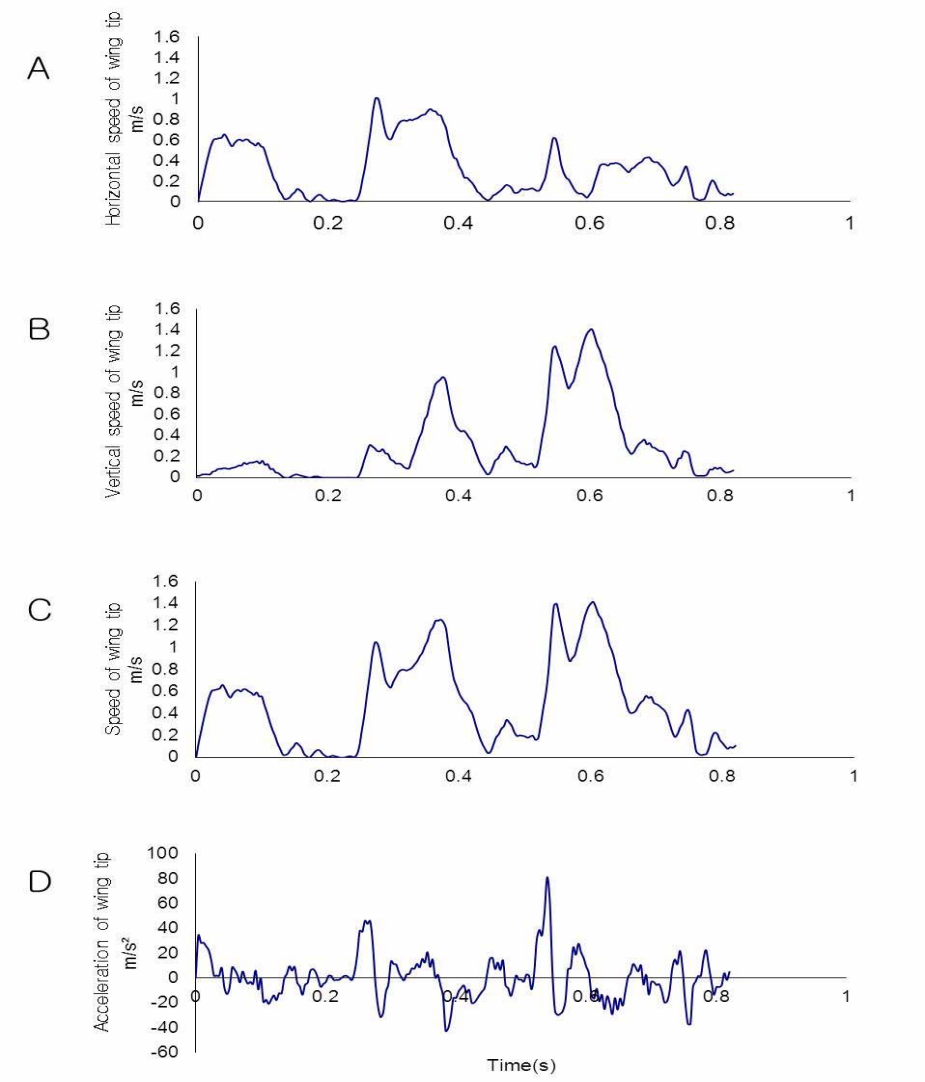


**Figure 25.** The horizontal (A) vertical (B) total (C) speed and total acceleration (d) of the robot wing tip movement in linear coordinates assuming that the wing expansion occurs in the two-dimnesional plane corresponding to the image in the high speed camera (250fps. lens: TV ZOOM LENS, M6Z 1212 – 3S, 12.5 – 75mm F1.2(www.edmundoptics.com)) is 1.8m). The left and right wing speeds were calcuated seperately and averaged. They were averaged again from the three recording video files. x-axis: time(s) y-axis: velocity(cm/s). D: acceleraton of wing tip based on the speed (C). x-axis: time(s) y-axis: acceleration(cm/s²).

### 3.3.4. Size, speed and accelaration between wing tips in the view of a prey

Angular size, expressed as distance between the wing tips in angular coordinates from the insect point of view, changed drastially in the intial part of the display (Figure 26A)

Angular speed remained zero during pause events and increased rapidly at every moment of display. It increased and decresed drastically in the first and second hitch but did not change much in the third hitch. When the movement reached the final movement (i.e. end of the display), the horizontal movement was much less pronounced than vertical movement. In the final part, the reason for showing the negaive values was that the tips were getting closer toward the end of the movement (Figure 26B).

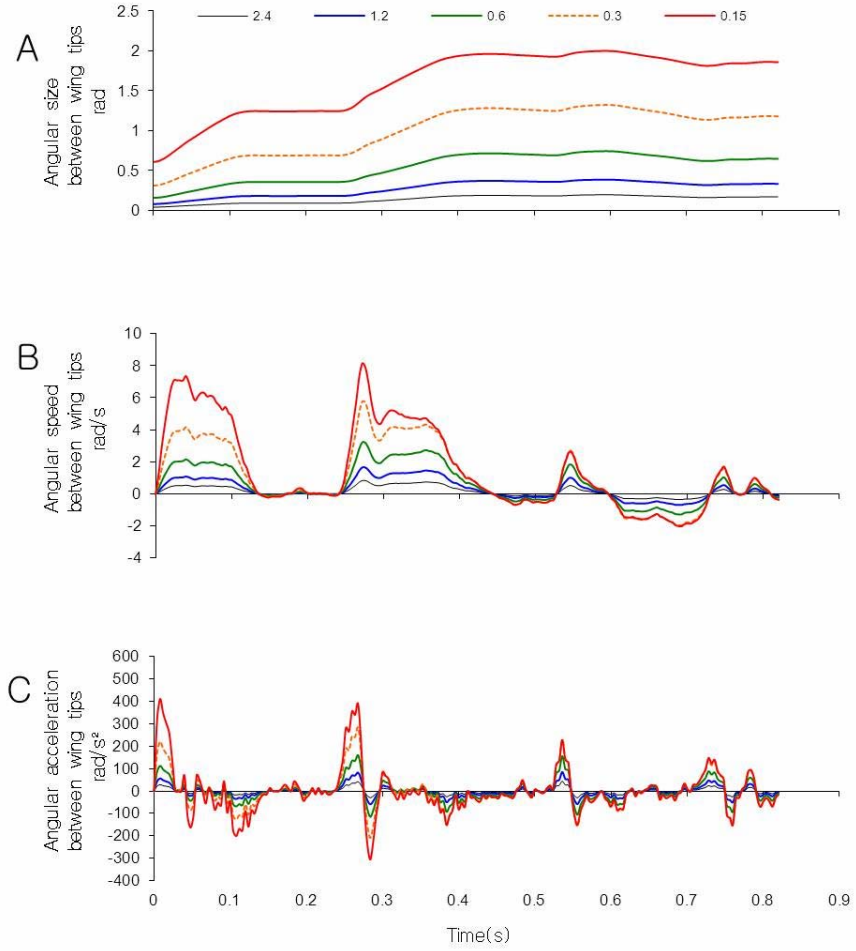


**Figure 26.** The distance between wing tips (A), speed (B) and acceleration (C) of wing expansion (change of distance per time unit) of the robot display represented in angular coordinates assuming that wing expansion occurs in the two-dimnesional plane corresponding to the image in the high speed camera (250fps. lens: TV ZOOM LENS, M6Z 1212 – 3S, 12.5 – 75mm F1.2; at 1.8m away from the robot) and that the grasshopper views this image from several distances (2.4m, 1.2m, 60cm, 30cm and 15cm). A: angular size between wing tips in the view of grasshopper in the display with 3 hitches. x-axis: time(s) y-axis: angle(radian) B: angular speed between wing tips in the view of a grasshopper in the display with 3 hitches. x-axis: time(s) y-axis: angular speed(radian/s) C: angular acceleration between wing tips in the view of a grasshopper in the display with 3 hitches. x-axis: time(s) y-axis: angulare acceleration(radian/s²)

### 3.3.5. Angular speed and acceleration according to a wing tip movement

As seen in the figure, the curve was separated into three parts corresponding to hitch events (Figure 27)

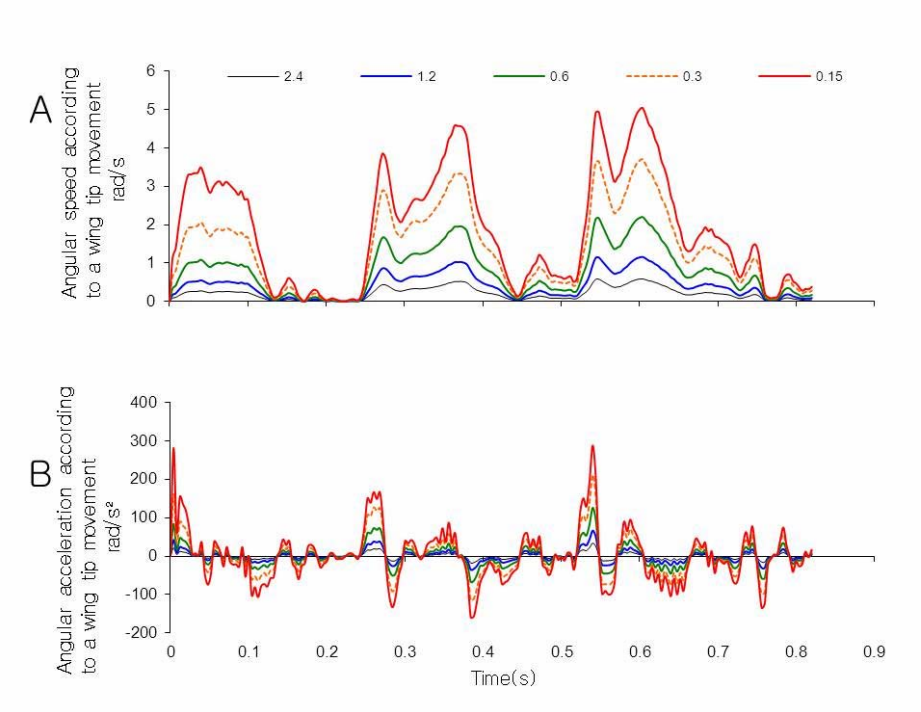


**Figure 27.** The total speed (A) and total acceleration (B) of the robot wing tip movement in angular coordinates assuming that the wing expansion occurs in the two-dimnesional plane corresponding to the image in the high speed camera (250fps. lens: TV ZOOM LENS, M6Z 1212 – 3S, 12.5 – 75mm F1.2; 1.8m away from the robot) and that the grasshopper views this image from several distances (2.4m, 1.2m, 60cm, 30cm and 15cm). The values from total three recording video files and were calculated in the view of a grasshopper in each distane (2.4, 1.2, 0.6, 0.3, 0.15m). A: angular speed based on a wing tip distance between former frame and later frame in the view of a grasshopper during the display with 3 hitches. The values were calculated from the distance between left and right wings. x-axis: time(s) y-axis: angular speed(radian/s) B: angular acceleration based on a wing tip distance between former frame and later frame in the view of a grasshopper in the display with 3 hitches. x-axis: time(s) y-axis: angular acceleration(radian/s²)

### 3.3.6. Spiking activity response to visual simulus

As shown in Figures 28~32, spikes were generated mostly in response to the movement of the robot, albeit with a noticeable delay of approximately 100-120 ms. However, due to natural situation and presence of wind induced movements in the background the spikes would also occur without apparent connection to the robot display.

Distance, and the correlated angular size and speed of the stimulus, clearly affected the response. There is hardly any response to robot displays at the distance 2.4 m between the insect and the robot (corresponding to the angular size of about 0.1 radians), and relatively weak response at the distance of 1.2m (corresponding to the angular size of about 0.2-0.3 radians). At the remaining smaller distances a clear pattern is visible: large portion of the spiking activity occurs in the time interval of a pause between hitches. Every moment of the 'pause', the spikes disappeared completely, but appeared again when the wing movement start, considering the response delay of 100-120 ms. This lead to three bursts of spike firing response to three hitches. The figure shows three time separate responses according to the stimuli. The third response was weaker than two earlier ones corresponding to wekaer stimulus in terms of the angular speed of wing tips expansion.

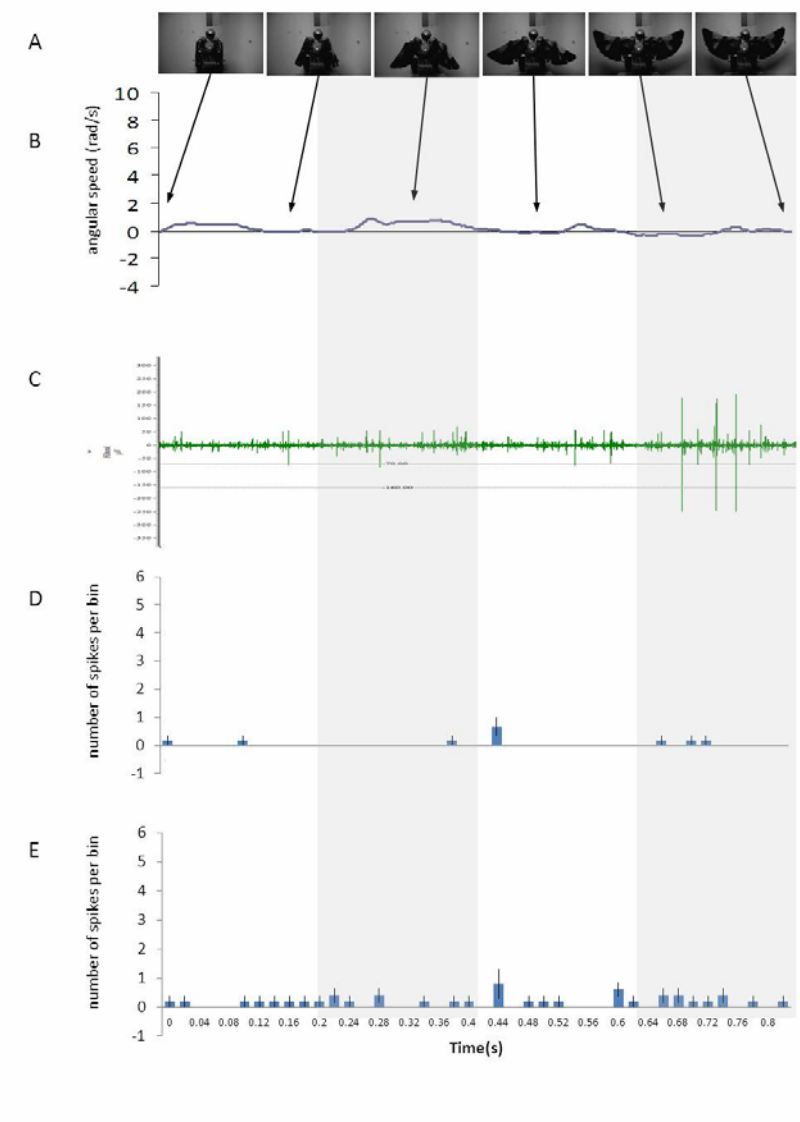


**Figure 28.** Spiking activity in response to the three-hitch display by the robot at a distance of 2.4m to the grasshopper A: Shchematics of the robot display, B: Angular speed between wing tips (radian/s), C: one example of a recorded response, D: Average number of spikes per bin (0.02s) counted by high threshold (n=7), E: Average number of spikes per bin counted by low threshold (n=5 adults) in 2011. Shaded stripes are drawn to help visual examination of timing of events in the various parts of the figure.

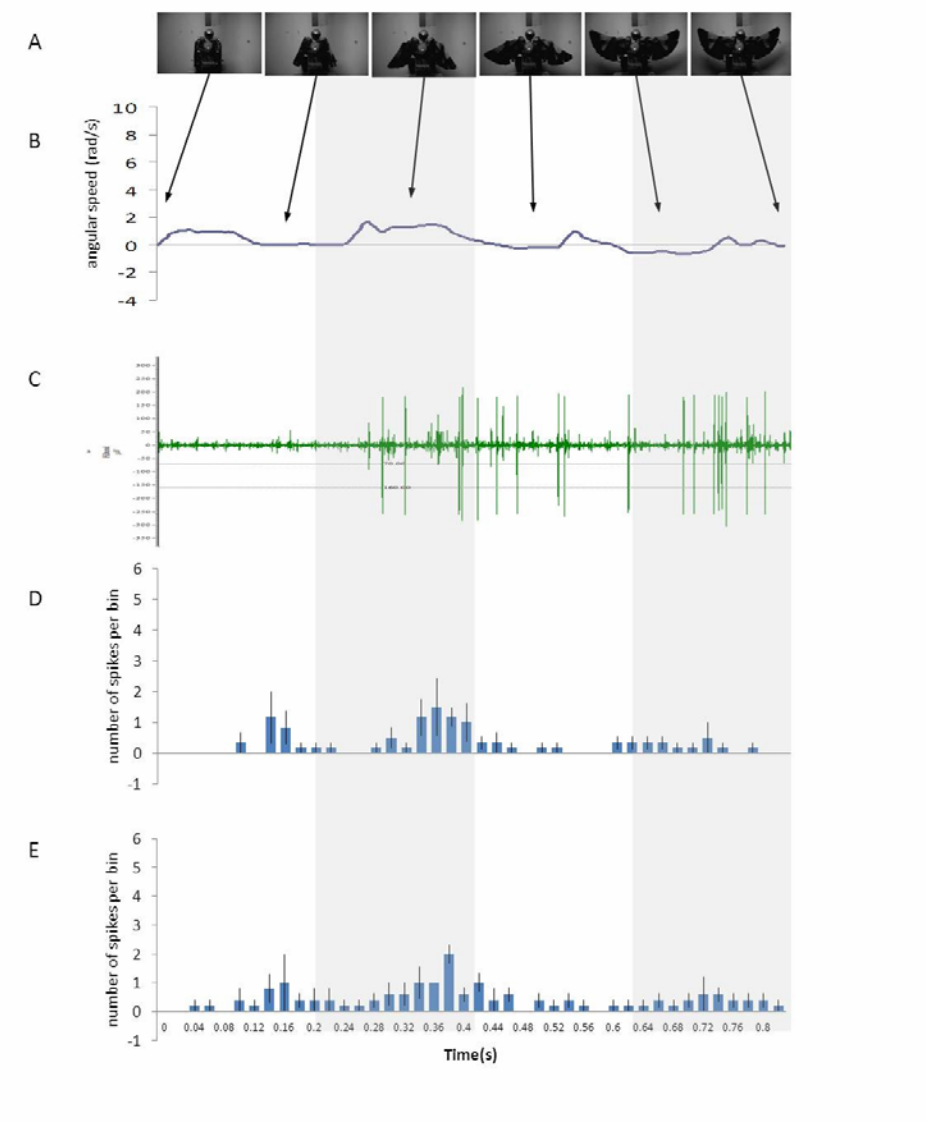


**Figure 29.** Spiking activity in response to the three-hitch display by the robot at a distance of 1.2m to the grasshopper A: Schematics of the robot display, B: Angular speed between wing tips (radian/s), C: one example of a recorded response, D: Average number of spikes per bin (0.02s) counted by high threshold (n=7), E: Average number of spikes per bin counted by low threshold (n=5 adults) in 2011. Shaded stripes are help visual examination of timing of events at the various parts of the figure.

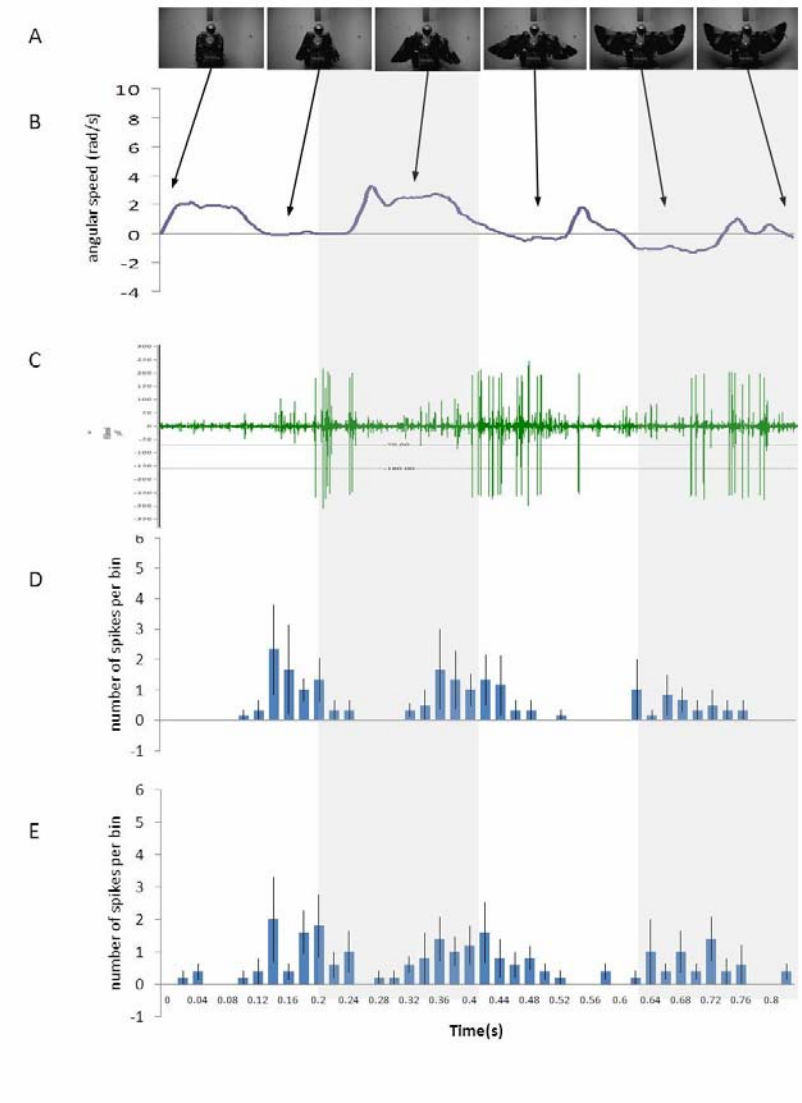


**Figure 30.** Spiking activity in response to the three-hitch display by the robot at a distance of 60cm to the grasshopper A: Shchematics of the robot display, B: Angular speed between wing tips (radian/s), C: one example of a recorded response, D: Average number of spikes per bin (0.02s) counted by high threshold (n=7), E: Average number of spikes per bin counted by low threshold (n=5 adults) in 2011. Shaded stripes are help visual examination of timing of events at the various parts of the figure.

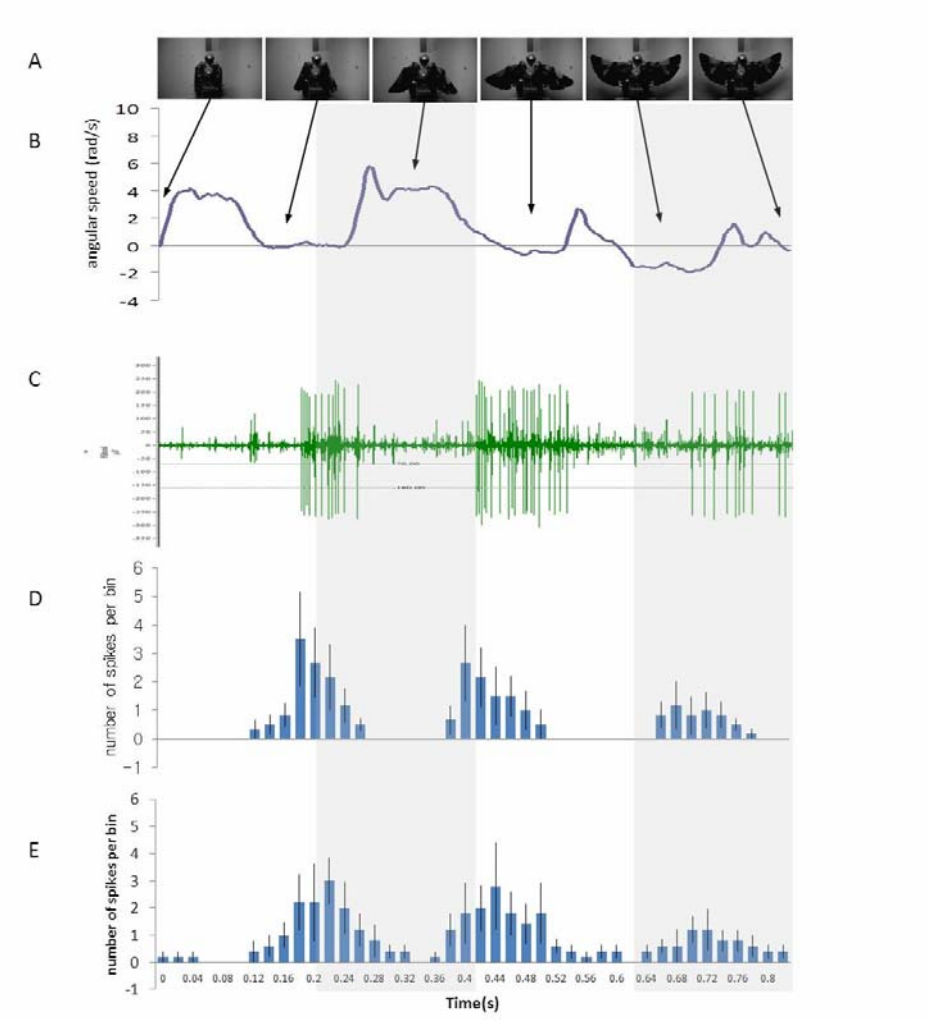


**Figure 31.** Spiking activity in response to the three-hitch display by the robot at a distance of 30cm to the grasshopper A: Shchematics of the robot display, B: Angular speed between wing tips (radian/s), C: one example of a recorded response, D: Average number of spikes per bin (0.02s) counted by high threshold (n=7), E: Average number of spikes per bin counted by low threshold (n=5 adults) in 2011. Shaded stripes are help visual examination of timing of events at the various parts of the figure.

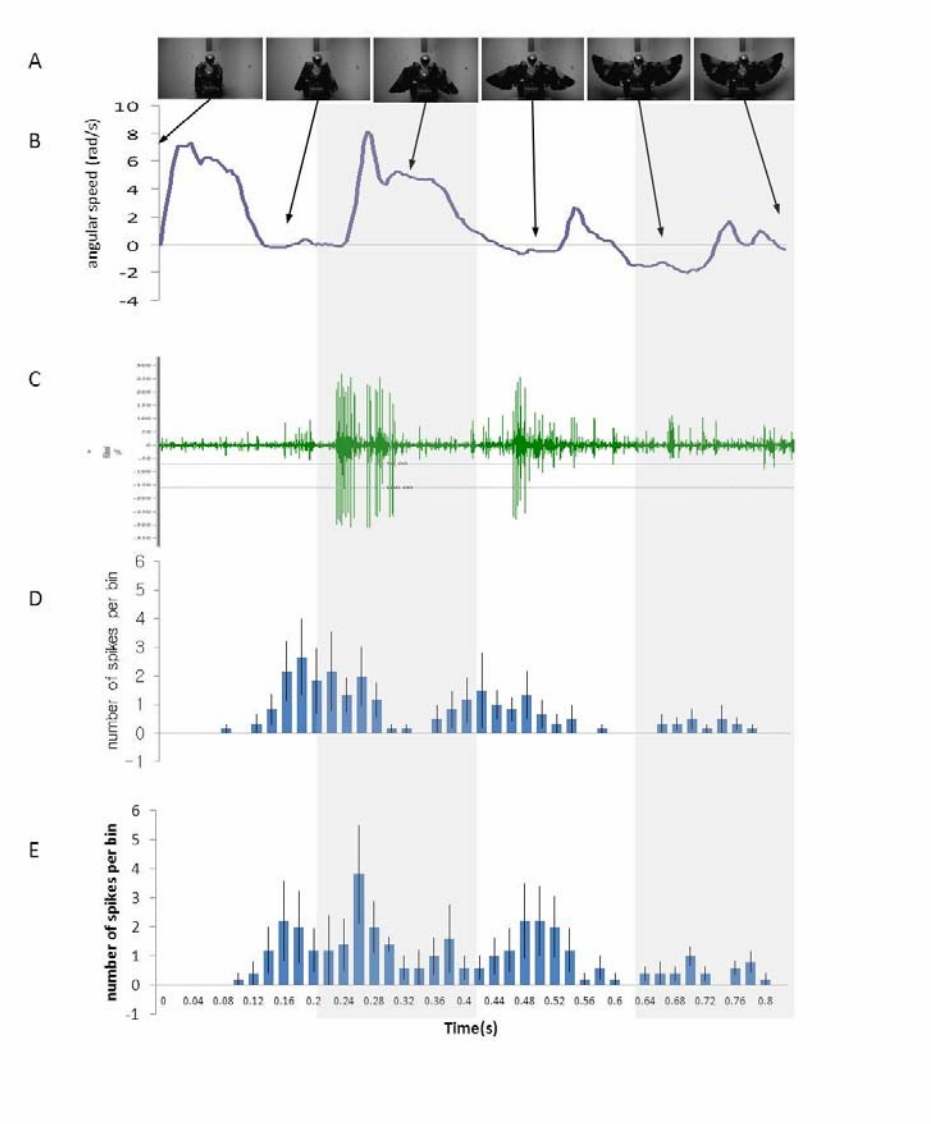


**Figure 32.** Spiking activity in response to the three-hitch display by the robot at a distance of 15cm to the grasshopper A: Shchematics of the robot display, B: Angular speed between wing tips (radian/s), C: one example of a recorded response, D: Average number of spikes per bin (0.02s) counted by high threshold (n=7), E: Average number of spikes per bin counted by low threshold (n=5 adults) in 2011. Shaded stripes are help visual examination of timing of events at the various parts of the figure.

## 3.4. Description of the full continuous wing movement by a robot and electrophysiological response of prey

### 3.4.1. Wing movement of robot mockingbird

The geometry of wing movemens is the same as the geometry during the three-hitch display. The only difference is timing: here the movment is continuous witthout pauses and therefore the display lasts shorter.

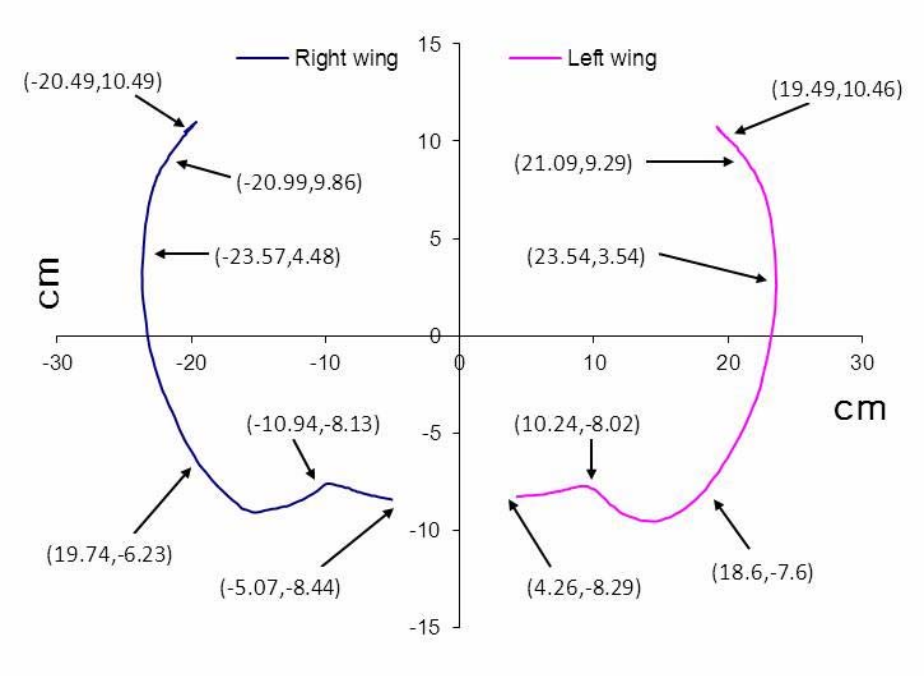


**Figure 33.** The movement of wing tips of the robot during continuous no –hitch display (left wing and right wings respectively). The numbers indicates x,y, coordinates of the wing tips (in cm) when I set the center of a robot (the white patch of Figure 3) area as the origin. The time interval between the marked coordinates is 27 frames. The time interval beween frames is 0.004 ms.

### 3.4.2. Distance between the left wing tip and the right wing tip

The speed of expansion between the two wing tips increased rapidy in the first 30ms and then the speed remained at the level of 1-2 m/s until about 200ms after which the speed decreased to zero (and became slightly negative) after 300ms from the display start (Figure 34B)

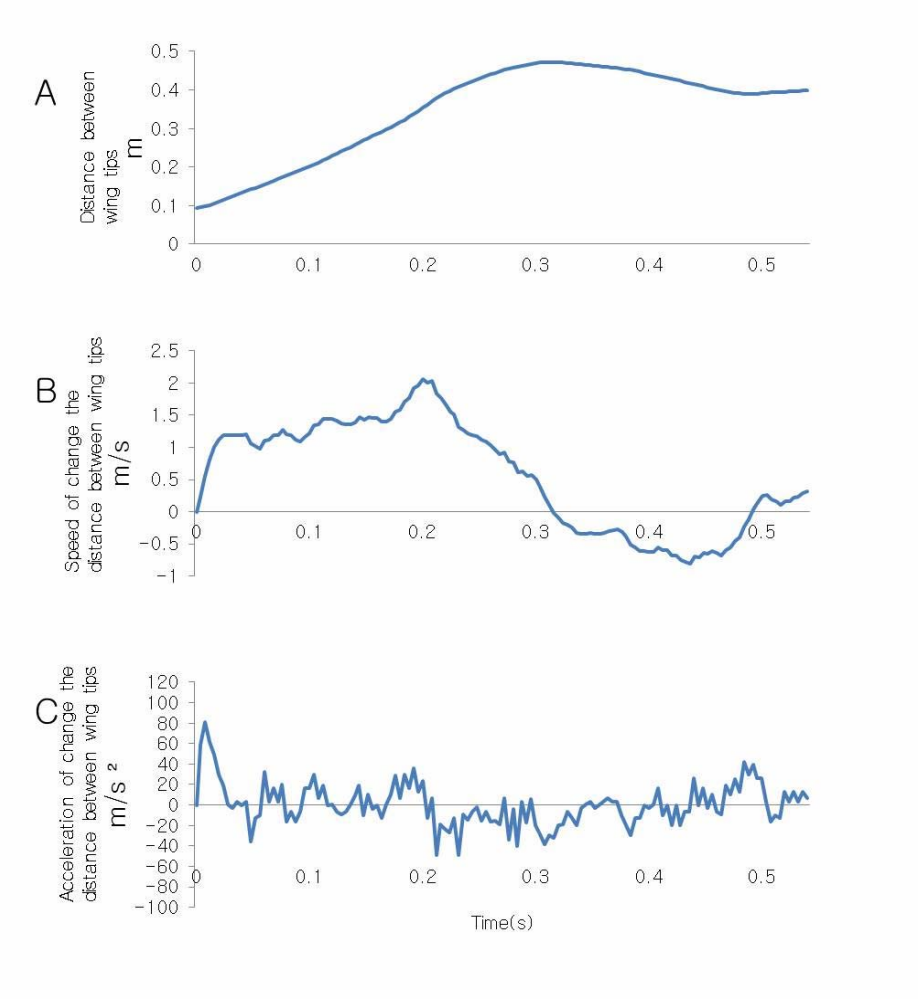


**Figure 34.** The distance between wing tips (A), speed (B) and acceleration (C) of wing expansion (change of distance per time unit) of the robot display represented in linear coordinates assuming that the wing expansion occurs in the two-dimnesional plane corresponding to the image in the high speed camera (250fps. lens: TV ZOOM LENS, M6Z 1212 – 3S, 12.5 – 75mm F1.2(www.edmundoptics.com)) is 1.8m. A: distance between the wing tips of robot with time. x-axis: time(s) y-axis: distance(cm) B: speed of change of distance between wing tips. x-axis: time(s) y-axis: speed(cm/s) C: acceleration of change of distance between wing tips. x-axis: time(s) y-axis: acceleration(cm/s²)

### 3.4.3. Coordinates of the wing tip according to time

The  coordinates were measured in the same manner as in the three-hitch display experiment. The wing opened continuously without hitches, so the duration was shorter and the curve was not seperated. Looking through the curve shape, the speed increased until some point then tendency to decrease in the speed is seen. (Figure 35)

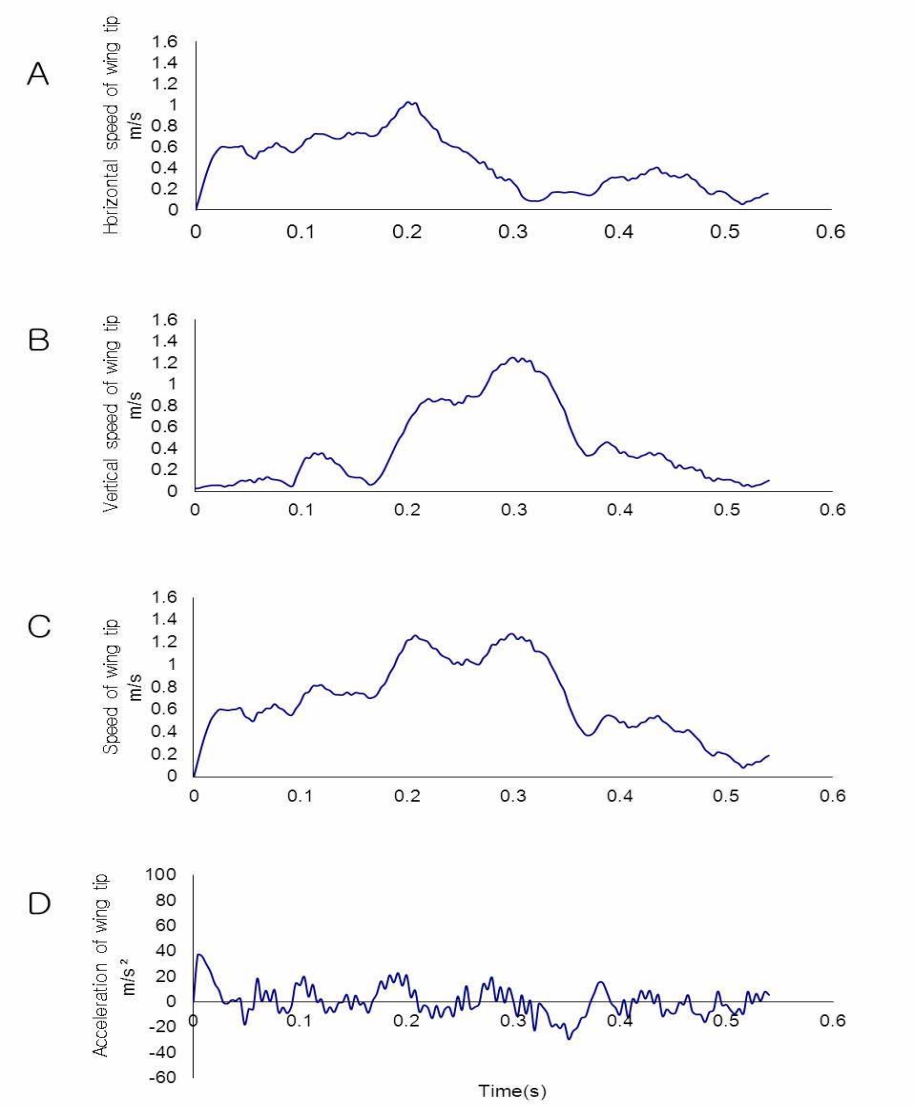


**Figure 35.** The horizontal (A) vertical (B) total (C) speed and total acceleration (d) of the robot wing tip movement in linear coordinates assuming that the wing expansion occurs in the two-dimnesional plane corresponding to the image in the high speed camera (250fps. lens: TV ZOOM LENS, M6Z 1212 – 3S, 12.5 – 75mm F1.2(www.edmundoptics.com)) is 1.8m). The left and right wing speeds were calcuated seperately and averaged. They were averaged again from the three recording video files. x-axis: time(s) y-axis: velocity(cm/s). D: acceleraton of wing tip based on the speed (C). x-axis: time(s) y-axis: acceleration(cm/s²).

### 3.4.4. Size, speed and accelaration between wing tips in the view of a prey

The shape of curve from the angular speed between wing tips was smooth unlike the curve in the experiment ‘with hitches’. (Figure 36B) During the time of the beginning movement, the speed increased dratiscally and then decreased gradually and it was negative during the final movement. This is because the wing tips are getting closer together at the end of the movement.

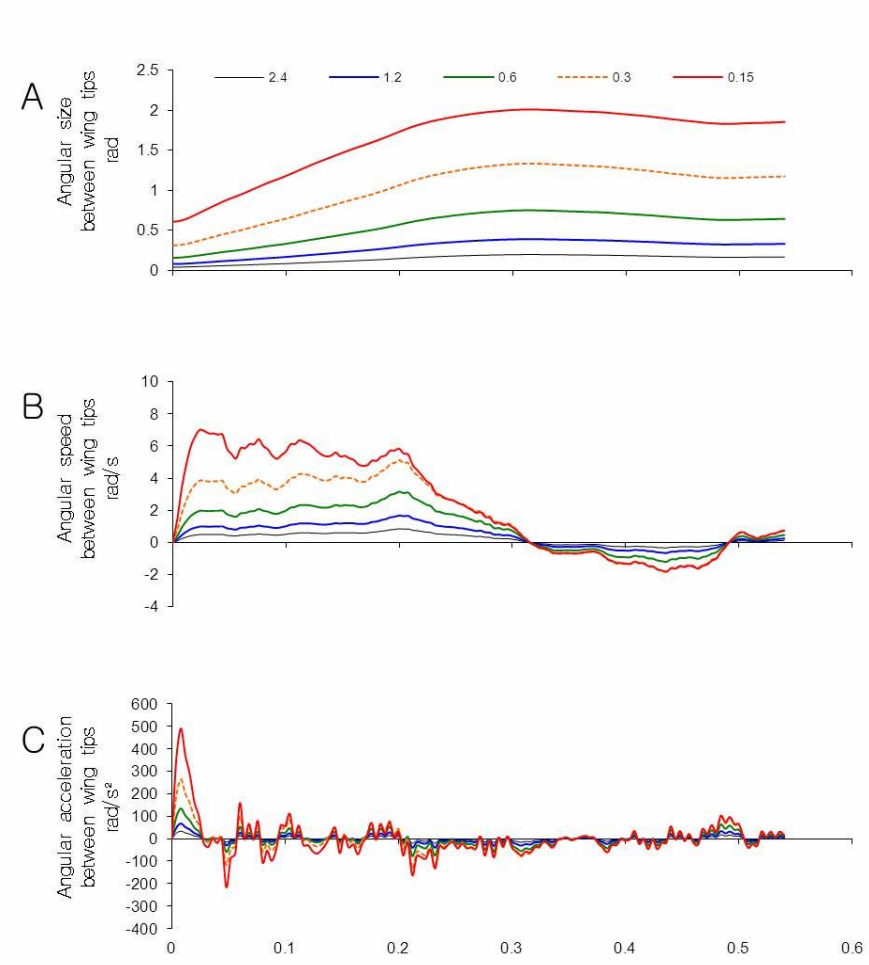


**Figure 36.** The distance between wing tips (A), speed (B) and acceleration (C) of wing expansion (change of distance per time unit) of the robot display represented in angular coordinates assuming that wing expansion occurs in the two-dimnesional plane corresponding to the image in the high speed camera (250fps. lens: TV ZOOM LENS, M6Z 1212 – 3S, 12.5 – 75mm F1.2; at 1.8m away from the robot) and that the grasshopper views this image from several distances (2.4m, 1.2m, 60cm, 30cm and 15cm). A: angular size between wing tips in the view of grasshopper in the display without hitches. x-axis: time(s) y-axis: angle(radian) B: angular speed between wing tips in the view of a grasshopper in the display without hitches. x-axis: time(s) y-axis: angular speed(radian/s) C: angular acceleration between wing tips in the view of a grasshopper in the display without hitches. x-axis: time(s) y-axis: angulare acceleration(radian/s²)

### 3.4.5. Angular speed and acceleration according to a wing tip movement

These values remain positive continuously in contrast to the three-hitch experiment.(Figure 37A). The highest angular speed (corresponding to the mot intense movements of edges across insect retina) is in the middle of the display, beween 200-400 ms, but the highest increase in the speed, corresponding to the highest acceleration of the image edges across retina of an insect is at the very beginning of the display.

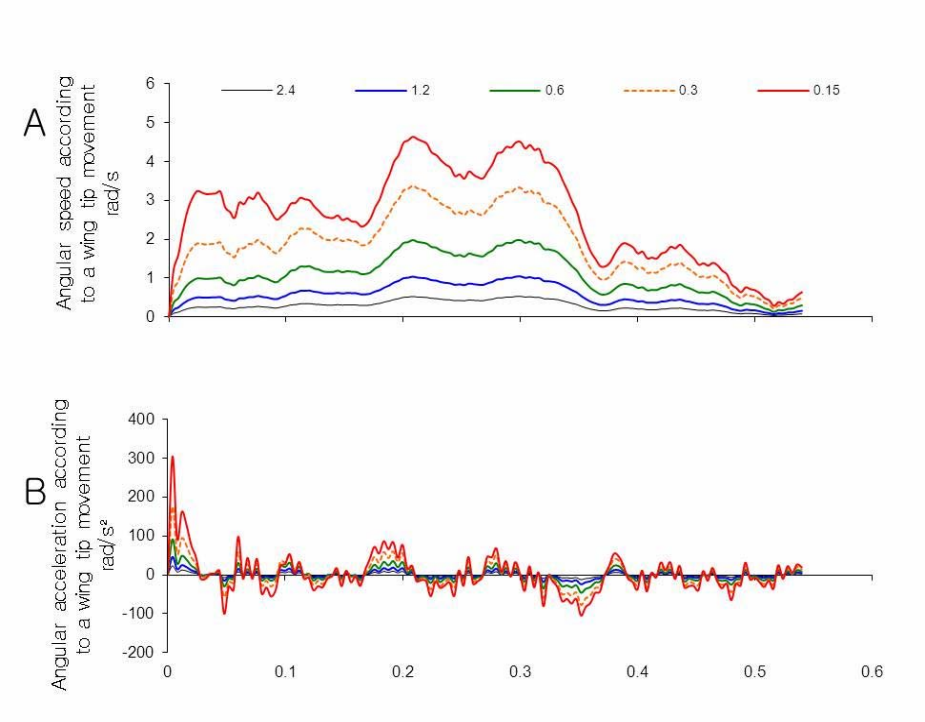


**Figure 37.** The total speed (A) and total acceleration (B) of the robot wing tip movement in angular coordinates assuming that the wing expansion occurs in the two-dimnesional plane corresponding to the image in the high speed camera (250fps. lens: TV ZOOM LENS, M6Z 1212 – 3S, 12.5 – 75mm F1.2; 1.8m away from the robot) and that the grasshopper views this image from several distances (2.4m, 1.2m, 60cm, 30cm and 15cm). The values from three video files were averaged. (A) - angular speed based on a wing tip distance between two consecutive frames in the video; x-axis: time(s) y-axis: angular speed(radian/s) B: angular acceleration based on (A); x-axis: time(s) y-axis: angular acceleration(radian/s²)

### 3.4.6. Spiking activity response to visual simulus

The figures show the DCMD response to the stimulus from the robot display without hitches. (Figure 38~42) From starting the movement of robot to end, the firing rate appeared continuously without any break period. The spikes formed smoothened curve in contrast with the curve from the experiment with hitch. However, like in the three-hitch experiment the distance, and the correlated angular size and speed of the stimulus, clearly affected the response. There was hardly any response to robot displays at the distance 2.4 m between the insect and the robot (corresponding to the angular size of about 0.1 radians), and relatively weak response at the distance of 1.2m (corresponding to the angular size of about 0.2-0.3 radians). At the remaining smaller distances a clear pattern is visible: the spiking starts 80-120ms after the display starts and starts dropping down after the angular speed of the stimulus drops.

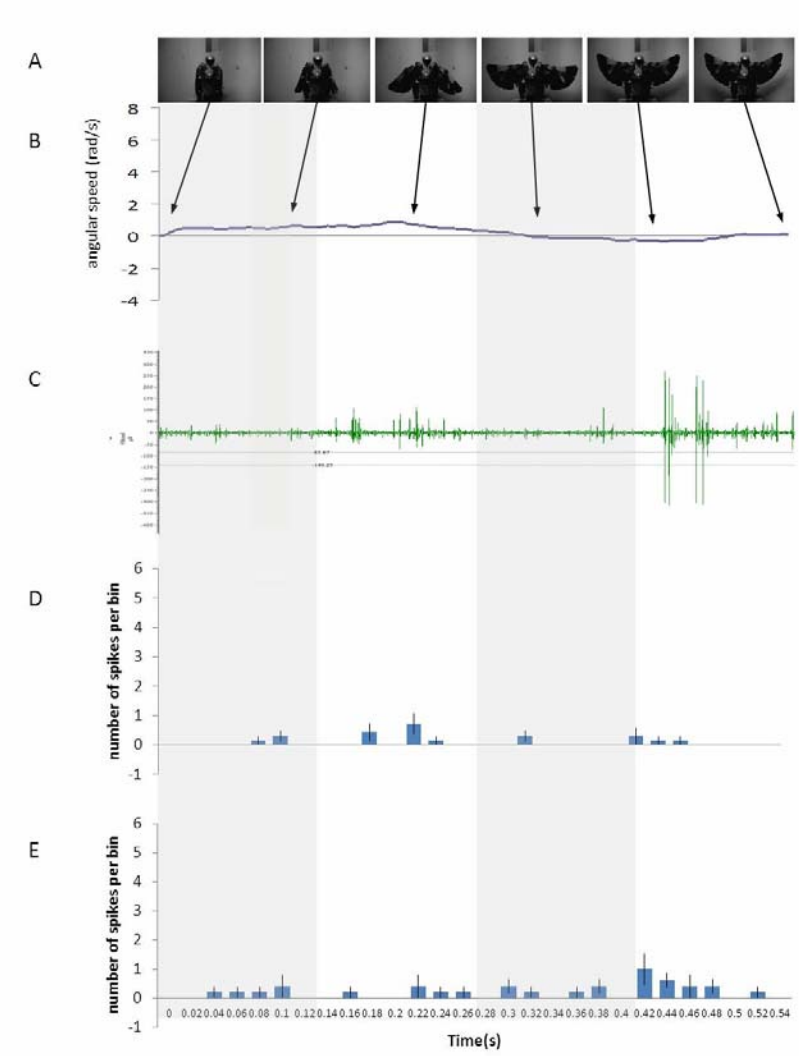


**Figure 38.** Spiking activity in response to the continuous no-hitch display by the robot at a distance of 2.4m to the grasshopper. A: Shchematics of the robot display, B: Angular speed between wing tips (radian/s), C: one example of a recorded response, D: Average number of spikes per bin (0.02s) counted by high threshold (n=7), E: Average number of spikes per bin counted by low threshold (n=5 adults in 2011). Shaded stripes are help visual examination of timing of events at the various parts of the figure.

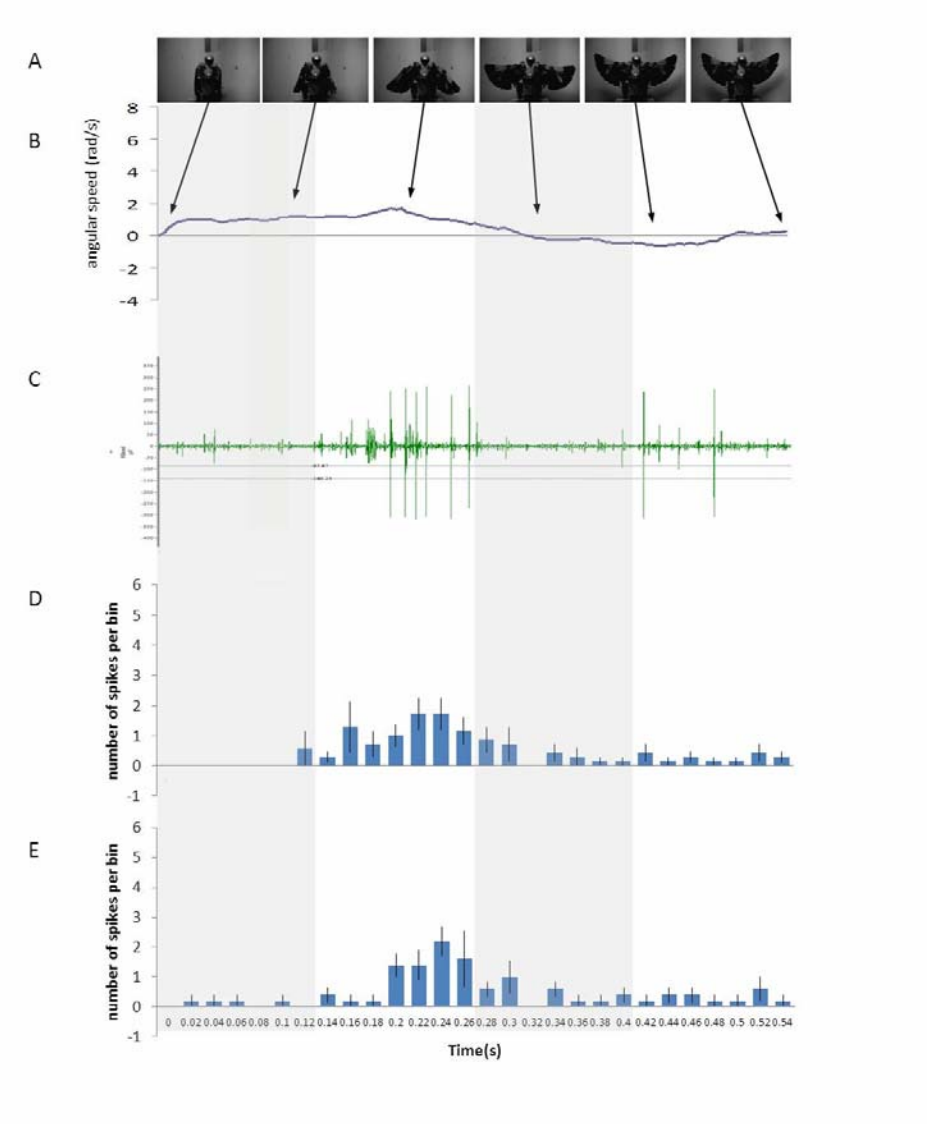


**Figure 39.** Spiking activity in response to the continuous no-hitch display by the robot at a distance of 1.2m to the grasshopper. A: Shchematics of the robot display, B: Angular speed between wing tips (radian/s), C: one example of a recorded response, D: Average number of spikes per bin (0.02s) counted by high threshold (n=7), E: Average number of spikes per bin counted by low threshold (n=5 adults) in 2011. Shaded stripes are help visual examination of timing of events at the various parts of the figure.

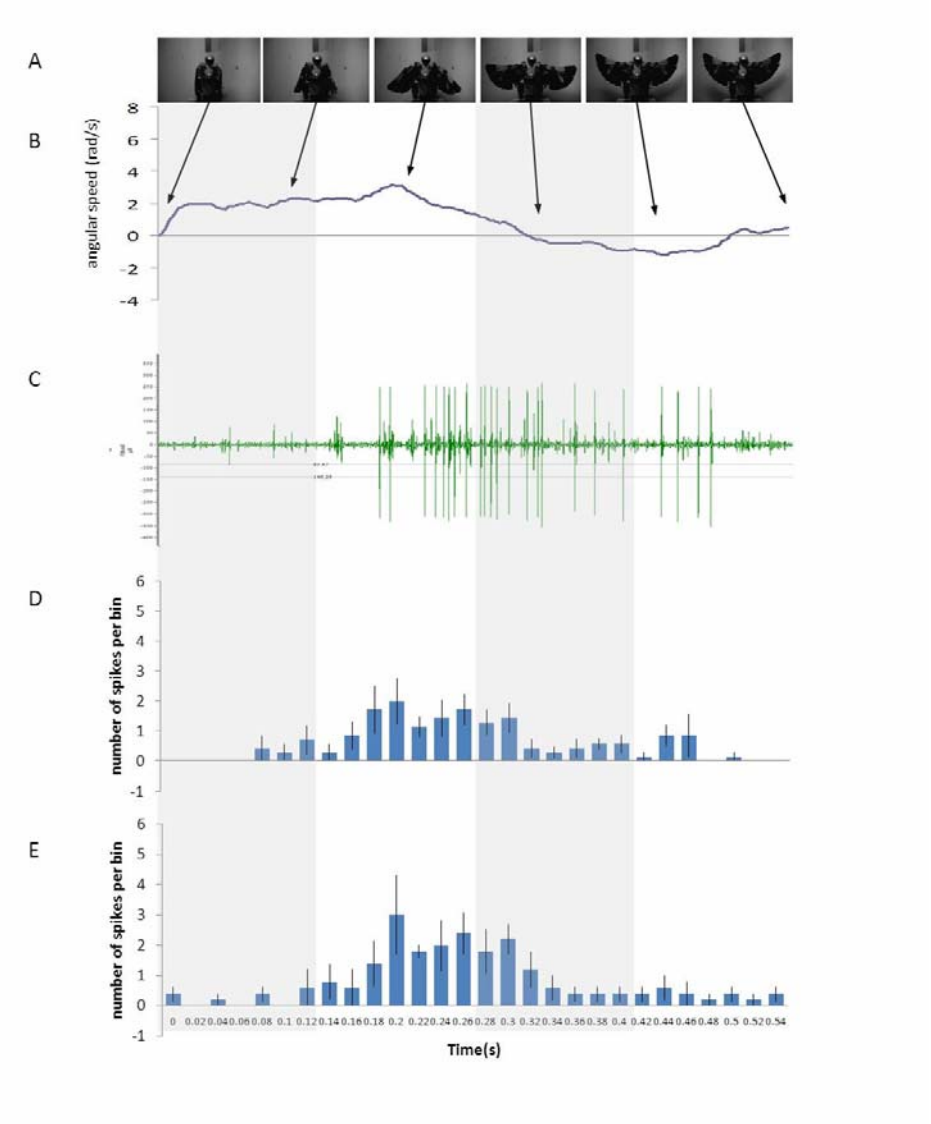


**Figure 40.** Spiking activity in response to the continuous no-hitch display by the robot at a distance of 60cm to the grasshopper. A: Shchematics of the robot display, B: Angular speed between wing tips (radian/s), C: one example of a recorded response, D: Average number of spikes per bin (0.02s) counted by high threshold (n=7), E: Average number of spikes per bin counted by low threshold (n=5 adults) in 2011. Shaded stripes are help visual examination of timing of events at the various parts of the figure.

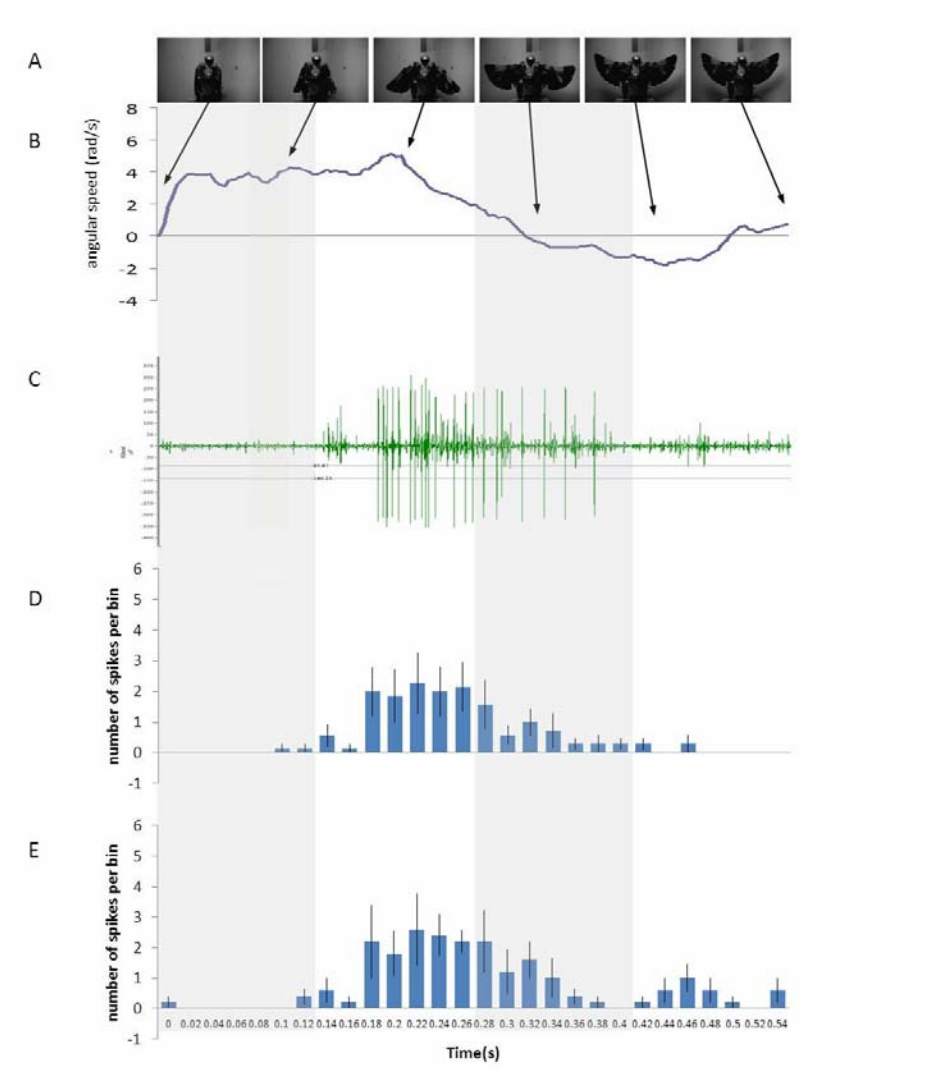


**Figure 41.** Spiking activity in response to the continuous no-hitch display by the robot at a distance of 30cm to the grasshopper. A: Shchematics of the robot display, B: Angular speed between wing tips (radian/s), C: one example of a recorded response, D: Average number of spikes per bin (0.02s) counted by high threshold (n=7), E: Average number of spikes per bin counted by low threshold (n=5 adults) in 2011. Shaded stripes are help visual examination of timing of events at the various parts of the figure.

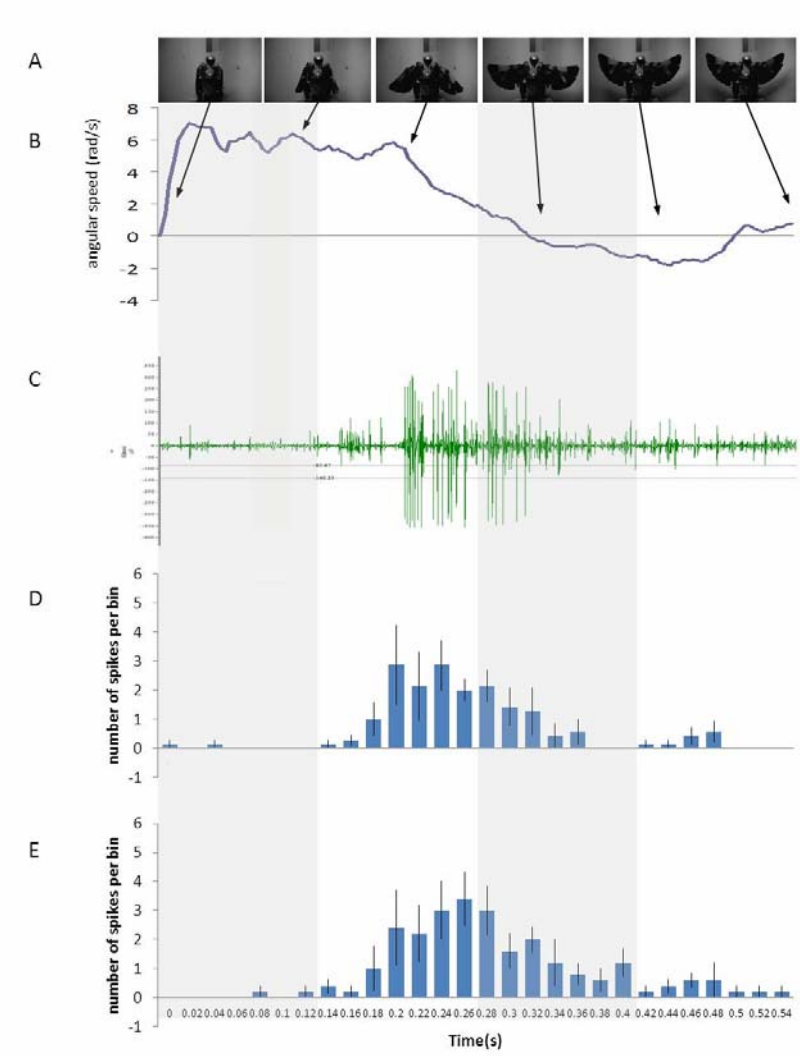


**Figure 42.** Spiking activity in response to the continuous no-hitch display by the robot at a distance of 15cm to the grasshopper. A: Shchematics of the robot display, B: Angular speed between wing tips (radian/s), C: one example of a recorded response, D: Average number of spikes per bin (0.02s) counted by high threshold (n=7), E: Average number of spikes per bin counted by low threshold (n=5 adults) in 2011. Shaded stripes are help visual examination of timing of events at the various parts of the figure.

# 4. Discussion

The results give us some insights and suggest new hypotheses on why the mockingbird display is composed of stereotypically performed hitches and pauses rather then being a full scale one time continuous wing opening movement. The robot experiments showed that the imitation of mockingbird wing flashing behavior with several hitches divided by paueses leads to approximately similar or even higher (e.g. compare for example Figure 31 with 41) maximal spiking intensity (at a gvien distance) as would do a single full wing flash. Hence, considering that escape is triggered when an increasing spiking activity in the LGMD/DCMD pathway crosses a specific threshold value (hypothesis proposed by one of the neurobiological groups studying the phenomenon; Rind 1984, Rind and Bramwell 1996, Rind and Santer 2004) there seems to be no need for the mockingbirds to peform a full scale wing flash in order to stimulate spiking activity that may be sufficient for triggering the escape reactions in the their orpthopteran prey. Therefore we predict that if this hypothesis is correct than behavioral experiments using the same robotic displays should show no difference in flushing grasshoppers between the no-hitch and three-hitch display.

Futhermore, my results indicate that the spiking occurs with a delay

(of roughly 80-120ms), which is generally consistent with previous litearture (Burrows 1996, Gray *et al.* 2001, Rind 1984, 1990, Rind and Bramwell 1996, Rind and Santer 2004, Rind and Simmons 1992, 1997).This leads to an additional hypothetical benefit of the three hitch display over the continuous display. The spiking activity in response to three hitch display largely occurs during the pauses (e.g. Figure 31, 32). Adding some additional time due to the delay in the motor neurons and reaction of muscles, we may predict that an escape may often be initiated during the pause, between the hitches. This prediction can be easily tested in behavioral experiments using the same robotic display and high speed video recording.

I hopothesize that it is benefcial for a bird to trigger the escape reactions during pauses between the wing movements because a bird, who is not involved in moving its wings, may be more ready to attack immediately and with better success. Therefore, I suspect that the relationship between the observed delay of the electrophysiological response (approximately 100 ms) and the duration of the one hitch display by a bird (also approximately 100ms) followed by one pause (also approximately 100 ms) are not coincidental. We propose that the stereotypical timing of the wingflash display is shaped natural selection for maximization of chances that the prey is flushed during by a pause which may lead to more successful chases after the prey. Finally, prey response to the three-hitch display apeared to be stronger (higher spiking

activity) as if the stimulus for triggering the escape (crossing a threshold of spiking actiivty) is amplified by inserting pauses within wing display. When I observed the pattern of spikes in a neuron response, grasshoppers expressed the most intense response when the stationary robot wings started to flash. Thus, I suggest that the the initial movement of the wing flashing may be an especially strong stimulus to induce escape behavior of the prey, maybe because the angular acceleartion is typically the largest during this time. Due to pauses seperating a wing flashing motion into several repeatedly initated steps, such an effect of initial stiumulus movement can be generated repeatedly.

When DCMD is activated, excitatory connections are made onto flexor and extensor motor neurons (Fotowat and Gabbiani 2007). So eventually the visual stimuli can trigger escape jumps (Guest and Gray 2006, Fotowat and Gabbiani 2007). Activation of escape circuit was affected by visual stimuli of looming object especially and the escape circuits are sensitive to the speed of image edge movements (Guest and Gray 2006). Thefore, when the robotic display was delivered far away from an insect (e.g. 2.4 m), and where consequently the angular speed of wing movement was low, the spiking activity was also low. As the distance to the robot decreased to 60cm the spiking activity increased and a pattern became clear. However the lack of further increase in spiking activity when the distance to the robot

decreased from 30 to 15 cm can be explained by the possibility that some of the stimulus was away from the main field of view of the grasshopper.

The effect of additional stimulus presented with wing flashing has been observed in other avian species. The previous studies showed that pivoting or vibrating behavior with wing flashing of Painted Redstart increased the escape distances (distance between predator and the preys location of escape) in several prey taxa group (Jablonski and Lee 2006, Jablonski and Strausfeld 2001). The DCMD neuron of orthopteron activity related to escaping (Jablonski and Lee 2006, Jablonski and Strausfeld 2001). . As flush-pursuing species, *Myioborus* redstart expose the white patches during stretching their wings and tail (Jablonski 1999, Jablonski et al 2006, Mumme et al 2006) and pivoting body movements affect preys' escape responses (Jablonski and Lee 2006, Jablonski and McInerney 2005, Jablonski and Strausfeld 2000). Therefore, I suggest that the mockingbird's white wing patches are also likely to help in flushing insect prey and future experiments with the robot may be used to test this hypothesis.

In conclusion, I showed that DCMD spiking occurs largely during pauses between hitches and I suggested that presence of pauses (and hitches) may be an adaptive feature of the wing dsiplay to increase efficiency flsuhing prey during the pauses, which may be important for increased pursue-capture success.

# References


Abrams, P. A. 1991. Strengths of indirect effects generated by optimal foraging. *Oikos* **62**: 167-176

Ali, S. 1962. *The birds of Sikkim*. Oxford University Press, Oxford.

Ali, S. 1977. *Field guide to the birds of the eastern Himalayas*. Oxford University Press, Oxford.

Ali, S. and Ripley, S. D. 1973a. *Handbook of the birds of India and Pakistan, vol. 8. Warblers to redstarts*. Oxford University Press, Oxford.

Ali, S. and Ripley, S. D. 1973b. *Handbook of the birds of India and Pakistan, vol. 9. Robins to Wagtails*. Oxford University Press, Oxford.

Batts, H. L. 1962. Wing-flashing motions in a catbird. *The Auk* **79**:112-113.

Beal, F. E. L. *et al.* 1941. *Common birds of Southeastern United States in relation to agriculturex*. U. S. Department of the Interior Fish and Wildlife Service Conservation Bulletin 15, United States government printing office, Washington.

Beehler, B. M. *et al.* 1986. *Birds of New Guinea*. Princeton Univerisity Press, Princeton, New Jersey.

Burrows, M. 1996. *The Neurobiology of an Insect Brain*. Oxford University Press, Oxford.

Burrows, M. 1995. Motor patterns during kicking movements in the locust.

*Journal of comparative physiology* **176**: 289-305.

Burrows, M. and Rowell, C. H. F. 1973. Connections between descending visual interneurons and metathoracic motoneurons in the locust. *Journal of comparative physiology* **85**: 221-234.

Burtt, E. H. *et al.* 1994. Wing-flashing in mockingbirds of the Galapagos Islands. *The Wilson Bulletin* **106**: 559-562.

Catania, K. C. 2008. Worm grunting, fiddling, and charming-humans unknowingly mimic a predator to harvest bait. *PLoS ONE* **3**: e3472

Catania, K. C. 2012. Evolution of brains and behavior for optimal foraging: A tale of two predators. *Proceedings of the National Academy of Sciences of the United States of America* **109**: 10701-10708.

Charnow E. L. *et al*. 1976. Ecological implications of resource depression. *The American Naturalist* **110**: 247-259.

Cramp, S. 1992. *Handbook of the birds of Europe, the Middle East and North Africa. The birds of the western Palearctic, vol. VI. Warblers*. Oxford University Press, Oxford.

Dawkins, R. and Krebs, J. R. 1979. Arms races between and within species. *Proceedings of the Royal Society of London. Series B, Biological Sciences* **205**: 489-511.

Dawkins, R. 1982. *The extended phenotype*. Oxford University Press, Oxford.

Dawson, J. W. *et al.* 2004. Acoustic startle/escape reactions in tethered flying locusts: motor patterns and wing kinematics underlying intentional steering.

*Journal of comparative physiology* **190**:581-600.

Derrickson, K. C. and Breitwisch, R. 2011. *The Birds of North America Online*: http://bna.birds.cornell.edu/bna/species/007. Cornell Laboratory of Ornithology 007, Ithaca. New York.

Dhondt, A. A. and Kemink, K. M. 2007. Wing-flashing in Northern mockingbirds: anti-predator defense? *Journal of Ethology* **26**: 361-365.

Ficken, M. S. and Ficken, W. R. 1962. The comparative ethology of the wood warblers: a review. *Living Bird* **2**:103-122.

Fleming, R. L. S. *et al.* 1979. *Birds of Nepal*. Kathmandu Avalok Publishers, Kathmandu.

Fotowat, H. and Gabbiani, F. 2007. Relationship between the phases of sensory and motor activity during a looming-evoked multistage escape behavior. *The Journal of Neuroscience* **27**: 10047-10059.

Gabbiani, F. *et al.* 2002. Multiplicative computation in a visual neuron sensitive to looming. *Nature* **420**: 320-324.

Gabbiani, F. *et al.* 2004. Muliplication and stimulus invariance in a looming-sensitive neuron. *Journal of Physiology* **98**: 19-34.

Gabbiani, F. *e al.* 2005. Time-dependent activation of feed-forward inhibition in a looming-sensitive neuron. *Journal of Neurophysiology* **94**: 2150-2161.

Gabbiani, F. and Krapp, H. G. 2006. Spike-frequency adaptation and intrinsic properties of an identified, looming-sensitive neuron. *Journal of Neurophysiology* **96**: 2951-2962.

Galatowitsch, M. L. and Mumme, R. L. 2004. Escape behavior of neotropical homopterans in response to a flush-pursuit predator. *Biotropica* **36**: 586-595.

Gray, J. R. *et al.* 2001. Activity of descending contralateral movement detector neurons and collision avoidance behavior in response to head-on visual stimuli in locusts. *Journal of comparative physiology* **187**: 115-129.

Guest, B. B. and Gray, J. R. 2006. Response of a looming-sensitive neuron to compound and paired object approaches. *Journal of Neurophysiology* **95**:1428-1441.

Hailman, J. P. 1960. A field study of the mockingbird's wing-flashing behavior and its association with foraging. *The Wilson Bulletin* **72**:346-357.

Halle, L. J. 1948. The Calandria mockingbird flashing its wings. *The Wilson Bulletin* **60**:243.

Hatsopoulos, N. *et al.* 1995. Elementary computation of object approach by a wide-field visual neuron. *Science* **270**: 1000-1003.

Haverschmidt, F. 1953. Wing-flashing of the Graceful mockingbird, Mimus gilvus. *The Wilson Bulletin* **65**:52.

Hayslette, S. E. 2003. A test of the foraging function of wing-flashing in northern mockingbirds. *Southeastern Naturalist* **2**: 93-98.

Hedenstrom, A. and Rosen, M. 2001. Predator versus prey: on aerial hunting and escape strategies in birds. *Behavioral Ecology* **12**: 150-156.

Heitler, W. J. and Fraser, K. 1993. Thoracic connections between crayfish giant fibres and motor giant neurons reverse abdominal pattern. *The*

*Journal of Experimental Biology* **181**: 329-333.

Hendricks, P. and Hendricks, L. M. 2006. Foot paddling by western gulls. *Northwestern Naturalist* **87**: 246-247.

Horwich, R. H. 1965. An ontogeny of wing-flashing in the mockingbird with reference to other behaviors. *The Wilson Bulletin* **77**: 264-281.

Hundley, M. H. 1963. Wing-flashing in the Galapagos mockingbird. *The Auk* **80**:372.

Jablonski, P. G. 1999. A rare predator exploits prey escape behavior: the role of tail-fanning and plumage contrast in foraging of the painted redstart (*Myioborus pictus*). *Behavioral Ecology* **10**: 7-14.

Jablonski, P. G. 2002. Searching for conspicuous versus cryptic prey: search rates of flush-pursuing versus substrate-gleaning birds. *The Condor* **104**: 657-661.

Jablonski. P. G. and Lee, S. D. 2006. Effects of visual stimuli, substrate-borne vibrations and air current stimuli on escape reactions in insect prey of flush-pursuing birds and their implications for evolution of flush-pursuers. *Behaviour* **143**: 303-324.

Jablonski, P. G. and McInerney, C. 2005. Prey escape direction is influenced by the pivoting displays of flush-pursuing birds. *Ethology* **111**: 381-396.

Jablonski, P. G. and Strausfeld, N. J. 2000. Exploitation of an ancient escape circuit by an avian predator: prey sensitivity to model predator display in the field. *Brain, Behavior and Evolution* **56**: 94-106.

Jablonski, P. G. and Strausfeld, N. J. 2001. Exploitation of an ancient escape circuit by an avian predator: relationships between taxon-specific prey escape circuits and the sensitivity to visual cues from the predator. *Brain, Behavior and Evolution* **58**:218-240.

Jablonski, P. G. *et al*. 2006. Habitat-specific sensory-exploitative signals in birds: propensity of dipteran prey to cause evolution of plumage variation in flush-pursuit insectivores. *Evolution* **60**: 2633-2642.

Judge, S. and Rind, F. C. 1997. The locust DCMD, a movement-detecting neurone tightly tuned to collision trajectories. *The Journal of Experimental Biology* **200**: 2209-2216.

Kaufmann, J. H. 1986. Stomping for earthworms by wood turtles, clemmys insculpta: a newly discovered foraging technique. *American Society of Ichthyologists and Herpetologists* **1986**: 1001-1004.

Laskey, A. R. 1962. Breeding biology of mockingbirds. *The Auk* **79**: 596-606.

MacKinnon, J. and Phillips, K. 1993. *A field guide to the birds of Borneo, Sumatra, Java and Bali*. Oxford University Press, Oxford.

Magurran, A. E. 1990. The inheritance and development of minnow anti-predator behaviour. *Animal Behaviour* **39**: 834-842.

Matsuda, H. *et al*. 1993. The effect of adaptive anti-predator behavior on exploitive competition and mutualism between predators. *Oikos* **68**: 549-559.

Matsuda, H. *et al*. 1996. Effects of predator-specific defence on

biodiversity and community complexity in two-trophic-level communities. *Evolutionary Ecology* **10**: 13-28.

Moynihan, M. 1962. The organization and probable evolution of some mixed species flocks of neotropical birds. *Smithsonian Misc Collection* **143**:1-140.

Mumme, R. L. *et al.* 2006. Evolutionary significance of geographic variation in a plumage-based foraging adaptation: an experimental test in the slate-throated redstart (Myioborus miniatus). *Evolution* **60**:1086-97.

Pizzey, G. 1980. *field guide to the birds of Australia*. Collins, Sydney.

Rich, T. D. 1980. Bilateral wing display in the sage thrasher. *The Wilson Bulletin* **92**: 512-513.

Ridgley, R. S. and Tudor, G. 1989. *The birds of South America, vol. I. The oscine passeriformes*. University of Texas Press, Austin, Texas.

Rind, F. C. 1984. A chemical synapse between two motion detecting neurones in the locust brain. *The Journal of Experimental Biology* **110**: 143–167.

Rind, F. C. 1990. Identification of directionally selective motion-detecting neurones in the locust lobula and their synaptic connections with an identified descending neurone. *The Journal of Experimental Biology* **149**: 21–43.

Rind, F. C. and Bramwell, D. I. 1996. A neural network based on the input organisation of an identified neuron signalling impending collision.

*Journal of Neurophysiology* **75**: 967–985.

Rind, F. C. and Santer, R. D. 2004. Collision avoidance and a looming sensitive neuron: size matters but biggest is not necessarily best. *The Royal Society* **271**: S27-S29.

Rind, F. C. and Simmons, P. J. 1992. Orthopteran DCMD neuron: a reevaluation of responses to moving objects. I. Selective responses to approaching objects. *Journal of Neurophysiology* **68**: 1654-1666.

Rind, F. C. and Simmons, P. J. 1997. Signaling of object approach by the DCMD. neuron of the locust *Journal of Neurophysiology* **77**:1029-33.

Rind, F. C. and Simmons, P. J. 1999 Seeing what is coming: building collision-sensitive neurons *Trends in Neurosciences* **22**: 215-220.

Robinson, S. K. and Holmes, R. T. 1982. Foraging behavior of forest birds: the relationships among search tactics, diet and habitat structure. *Ecology* **63**:1918-1931.

Santer, R. D. *et al.* 2006. Role of an identified looming-sensitive neuron in triggering a flying locust's escape. *Journal of Neurophysiology* **95**:3391-3400.

Santer, R. D. *et al.* 2008. Preparing for escape: an examination of the role of the DCMD neuron in locust escape jumps. *Journal of Comparative Physiology A* **194**: 69-77.

Selander, R. K. and Hunter, D. K. 1960. On the functions of wing-flashing in mockingbirds. *The Wilson Bulletin* **72**:341-345.

Sherry, T. W. 1984. Comparative dietary ecology of sympatric, insectivorous neotropical flycatchers (Tyrannidae). *Ecological Monographs* **54**:319-338.

Simmons, P. J. 1981. Ocellar excitation of the DCMD: an identified locust interneurone. *The Journal of Experimental Biology* **91**: 355-359.

Simmons, P. J. and Rind, F. C. 1992. Orthopteran DCMD neuron: a reevaluation of responses to moving objects. II. Critical cues for detecting approaching objects. *Journal of Neurobiology* **68**: 1667-1682.

Simmons, P. J. *et al.* 2010. Escapes with and without preparation: the neuroethology of visual startle in locusts. *Journal of Insect Physiology* **56**: 876-883.

Tinbergen, N. 1960. *The herring gull's world: a study of the social behavior of birds*. Basic Books, New York.

Whitaker, L. M. 1957. Comments on wing-flashing and its occurrence in Mimidae with uniformly colored wings. *The Wilson Bulletin* **69**:361-363.

# 국문초록

군비경쟁을 통해 포식자와 피식자가 공진화하는 과정에서 일부 포식자는 피식자가 도주하는 행동을 이용하게 되었다. 몇 몇 새들은 갑자기 날개를 펴는 행동으로 숨어있는 곤충을 놀라게 해서 눈에 띄면 좇아가 잡아먹는데, 이 중 흉내지빠귀 (mockingbird) 에서 특이한 것은 날개를 펴는 도중 멈추는 순간을 몇 차례 섞는 것이다. 이런 행동이 포식율을 높일 것이라 가정한 본 연구에서는 실제 새를 닮은 로봇을 만들어 서식지인 미국의 아리조나주에서 효과를 확인해 보았다. 로봇의 동작은 실제 흉내지빠귀와 같이 멈춤동작을 하며 날개를 펴는 경우과 한 번에 날개를 펴는 경우 두가지로 나누었다. 이에 대한 피식자의 반응은, 아리조나 사막의 메뚜기들을 채집하여 시각자극에 반응하는 경로로 잘 알려진 DCMD 신경의 활성을 통해 살펴보았다. 결과를 분석해 본 결과, 메뚜기의 신경반응은 로봇으로부터 시각자극을 받은 후 시간이 약간 흐른 후 일어났는데, 이는 흉내지빠귀가 날개를 멈추는 시점과 일치한다. 날개를 멈추는 순간 도주반응이 일어나 피식자를 발견하게 된다면 즉시 좇아가기가 수월해 질 것을 예상할 수 있다. 반응의 강도는 시각자극이 처음 주어질 때 가장 크게 나타나는데, 멈춤 동작을 섞는다면 시작하는

시점을 다시금 만들어내게 되므로 도주반응이 최대가 되는 순간을 흉내지빠귀가 반복적으로 유도하고 있다고 볼 수 있다. 도주행동으로 연결되는 DCMD 의 활성은 기본적으로 다가오는 물체에 민감하다는 것이 많은 연구를 통해 알려져 있다. 본 연구는 흉내지빠귀가 날개를 펼쳐 몸을 확대함으로써 피식자에게 다가가는 듯한 효과를 줌과 동시에 기타 복합적인 효과들을 살려 포식율을 높여왔음을 시사하고 있다.

**주요어 : 군비경쟁, 공진화, 흉내지빠귀, 포식자, 도주, 신경**

**학　번 : 2010-23108**